Modular Synthesis Framework for Combined Separation/Reaction Systems

Soraya Rahim Ismail, Petros Proios, and Efstratios N. Pistikopoulos
Centre for Process Systems Engineering, Dept. of Chemical Engineering, Imperial College, London SW7 2BY, U.K.

As an extension to our earlier work (1999a), this article presents a systematic approach for the synthesis of combined separation/reaction systems which involves a phenomena-based representation formulated within a superstructure optimization framework. A multifunctional, mass-/heat-transfer-based process module is utilized as the building block of process alternatives. Within this module, Gibbs-free-energy-based "driving-force" constraints are introduced to describe the physiochemical phenomena and to ensure feasibility of pure separation, reaction or combined separation/reaction (such as reactive distillation). A superstructure of these multipurpose modules is then systematically constructed to represent process alternatives, which are not explicitly prepostulated, but investigated, as mass and heat exchange network possibilities.

Introduction

Successful application of novel hybrid units in the industrial production of chemicals such as MTBE has fueled academic interest in processes of integrated reaction and separation phenomena (Doherty and Buzad, 1992). However, advances in the modeling, design, and analysis of combined reaction and separation operations have been mainly concentrated on the specific case of reactive distillation. Reactive distillation is applied specifically to reversible chemical reactions in the liquid phase, whereby the conversion of reactants is limited by the reaction equilibrium. By combining two operations in one unit, reactive distillation allows synergistic effects to occur, for example, the shift of equilibrium by separation of the products, enhancing conversion by Le Chatelier's principle, and utilization of the reaction heat for the separation of educts and products. Other advantages include the suppression of undesired side reactions, and the ability to achieve high conversions at stoichiometric feed flow rates. As a result, capital cost, recycle operating cost, and utility costs are minimized due to the reduction in the number of processing units and direct heat integration between separation and reaction.

Advances in the analysis of reactive distillation have concentrated on the case of simultaneous chemical and physical equilibrium. These include the pioneering works of Doherty and coworkers who employed transformed variables (Barbosa and Doherty, 1988c; Ung and Doherty, 1995a; Okasinski and Doherty, 1997) and the elemental balance approach of Perez-Cisneros et al. (1997). Both these strategies reduce the system dimension, allowing the visualization of multicomponent reactive systems in two- or three-dimensional diagrams for direct analysis. In terms of design of reactive distillation columns—that is, the determination of feasible design parameters such as reflux ratios and the number of stages that can achieve the desired product specifications for given inputs—two main approaches prevail; graphical fixed point methods, and mixed integer nonlinear programming (MINLP) approaches. The fixed point methods are based on the use of transformed variables, which when assuming chemical and physical equilibrium, are restricted to columns with reaction occurring on every stage (Barbosa and Doherty, 1988a; Ung and Doherty, 1995b). When reaction kinetics with physical equilibrium is considered, the combination of reactive and nonreactive zones can be accounted for. However, these procedures are currently restricted to single reaction systems, in single feed columns (Okasinski and Doherty, 1998). The MINLP approaches which utilize a superstructure scheme are readily applicable to multicomponent, multireaction systems in multifeed columns. These use reaction kinetics, can consider heat effects, and can result in an optimal reactive column with respect to cost (Ciric and Gu, 1994; Smith, 1996).

In terms of nonequilibrium models, Higler et al. (1998) recently presented a simulation model for a single feed reactive

Correspondence concerning this article should be addressed to E. N. Pistikopoulos.

column, utilizing reaction kinetics and accounting for the coupling between chemical reaction and mass transfer. On a more conceptual level, Hauan and Lien (1998) take on a different approach and present an analytical framework for reactive distillation systems based on the notion of phenomena vectors (see also Hauan, 1998). Rather than process alternatives, this provides synthesis targets. Similarly, for the synthesis of general reaction-separation systems, standard configurative approaches focus on providing synthesis targets rather than deriving alternatives (Lakshmanan and Biegler, 1996; Nisoli et al., 1997).

Although a much greater understanding of combined reaction separation systems have been gained, in terms of *synthesis*, there are still no generally accepted procedures for the generation of hybrid reactive/separation possibilities. In this article, a phenomena based modeling framework that is able to capture hybrid reactive/separation possibilities is presented. In this framework, we are utilizing a multifunctional process module, which is based on fundamental mass- and heat-transfer principles. This allows for the generation of process alternatives without explicitly prepostulating a superstructure of units.

The synthesis problem is formally stated. The mass-/heat-transfer module which constitutes the basis for the synthesis representation is then described. The corresponding mass-transfer constraints are derived for general nonideal mixtures and a simulation study analyzes them. The synthesis framework is presented and the resulting superstructure model is detailed. Finally, synthesis examples are considered.

Problem Statement

The synthesis problem can be stated as follows:

Given

- A set of feedstreams of given composition (their flow rates and temperatures could also be given or could be included as additional optimization variables).
- A set of desired products with specifications on flow rate, temperature and purity.
- A set of available mass utilities such as catalysts and mass exchange agents.
- A set of available heat utilities such as cooling water and steam and specifications on availability, supply temperatures and compositions.
- All reactions schemes and kinetics data.
- Cost data of feeds and utilities.
- All thermodynamic property models.

Synthesize an 'optimal' process system, that is, sequence of reactors and/or separators. In this work, the system cost is comprised of utilities, cost of raw materials, and an approximation of capital costs based on the number of mass/heat separator and reactor blocks. At this point, a note must be made regarding the word 'optimal' above. The latter is written throughout this publication in quotation marks for consistency reasons due to the approximating capital cost model utilized (discussed further later) and to the fact that the problem is not solved to global optimality. The synthesis problem addressed in this article is applicable to systems whereby reaction, separation, and combined reaction and separation can take place. The basic assumptions in this work are that (i) there is no liquid/liquid equilibrium, (ii) reactions occur in the liquid phase only, and (iii) there is no heat integration between the heaters and coolers. Extension of the framework to relax (i) and (ii) is under current investigation. Assumption (iii), however, is not a limitation of the approach and can be relaxed at the cost of increased model size as discussed in the later sections.

For illustrative purposes in the following sections, consider the process synthesis for the production of 99% pure liquid methyl acetate (D) required at a rate of 10 kmol/h given as feedstreams pure saturated liquid acetic acid A and methanol B. The following reversible reaction occurs

$$A + B \rightleftharpoons C + D \tag{1}$$

and sulfuric acid is available as catalyst to enhance the forward reaction. Cooling water CW and steam St are available as cooling and heating utilities.

Mass-/Heat-Transfer Module and Representation

A process operation can be generally characterized by a set of mass- and heat-transfer phenomena, where the mass transfer of a component from one substance or phase to another due to a difference in chemical potential takes place. Based on this concept, a two-exchanger module, as introduced in our earlier work (Papalexandri and Pistikopoulos, 1996), is utilized to form the building block of process alternatives. The mass/heat exchange block as shown in Figure 1a consists of a mass/heat exchange module, where mass and heat transfer takes place between the participating streams, and a pure heat exchange module, where streams do not come into "mass active" contact. Side mixers and splitters are assigned to each mass/heat exchange and pure heat exchange module, and block-superstructure rules are applied allowing

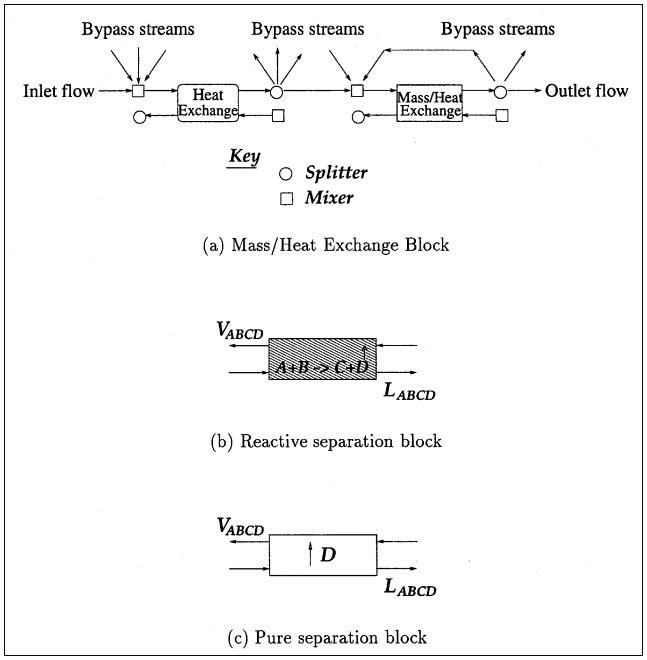

Figure 1. Mass/heat exchange modules.

for all possible interconnections between exchangers. An initial splitter is also considered for each possible feedstream, and a final mixer for each possible initial, intermediate, and final stream.

As process operations are viewed as sets of mass and heat exchange, process units can be realized by sets of properly connected mass and heat exchange blocks. Combined separation and reaction hybrid processes are represented by sets of connected modules whereby the correct phenomena are occurring. Consider, for example, the production of methyl acetate D from an equimolar feed of acetic acid A and methanol B by reaction 1 as described in the previous section in a double feed reactive distillation column. A reactive distillation tray involves mass and heat transfer within the liquid holdup due to reaction in addition to mass and heat transfer between the liquid and vapor mixtures (represented by L_{ABCD} and V_{ABCD}) due to volatility differences (Figure 1b). On a nonreactive tray with only separation (Figure 1c), mass and heat transfer occurs between the liquid and vapor contacting phases of a mixture. The reactive column is thus realized as a configuration of modules, as illustrated in Figure 2a. The feeds enter the mixers of the mass/heat exchangers, the acetic acid as a liquid and the methanol as a vapor. The two liquid-vapor modules between the feeds represents the reactive section of the column where the bulk of the reaction occurs. In this section, reaction occurs in the liquid holdup of the module and the continual removal of the reaction products C and D drives the reaction forwards. Note that the order of relative volatility is $D > B > C > A$; thus, overall we have mass transfer of D from the liquid to the vapor phase, and transfer of component C from the vapor phase to the liquid phase. The top $L_{\mathrm{ABCD}} - V_{\mathrm{ABCD}}$ mass/heat exchange block has no liquid holdup, representing the rectifying section, whereby D is transferred from the liquid to the vapor stream and ABC is transferred from the vapor to the liquid stream. The bottom module has little/no reaction due to a low concentration of A and no holdup, and represents the stripping section whereby water C is transferred to the liquid stream while methanol B is transferred to the vapor stream. The condenser is realized as a pure heat-transfer block between an inlet vapor stream and a cooling utility, whereby thermodynamic constraints ensure that the inlet stream is of vapor phase which is cooled to a liquid outlet stream. Similarly, a reboiler is realized as heat exchange between a hot utility stream and an inlet liquid phase stream which is heated to a vapor phase. Here, each *liquid-vapor* mass/heat exchanger represents an aggregate of distillation trays.

For the general synthesis problem for the production of D, alternative process structures featuring different operating conditions may result depending on the synthesis objective. Figure 2b show a conventional alternative, featuring reaction in the liquid phase up to equilibrium followed by separation of D from the resulting mixture. Within each liquid-liquid module, mass/heat exchange occurs between a liquid reagent stream and a liquid reaction product stream which are assumed to be well mixed in order to define the reaction kinetics. Since each module corresponds to a continuous stirred tank reactor (CSTR), the series of modules represent a plug-flow reactor (PFR). The proceeding liquid-vapor modules separate the desired product from reactor exit stream, representing a separation column similar to the reactive column of Figure 2a with no reaction.

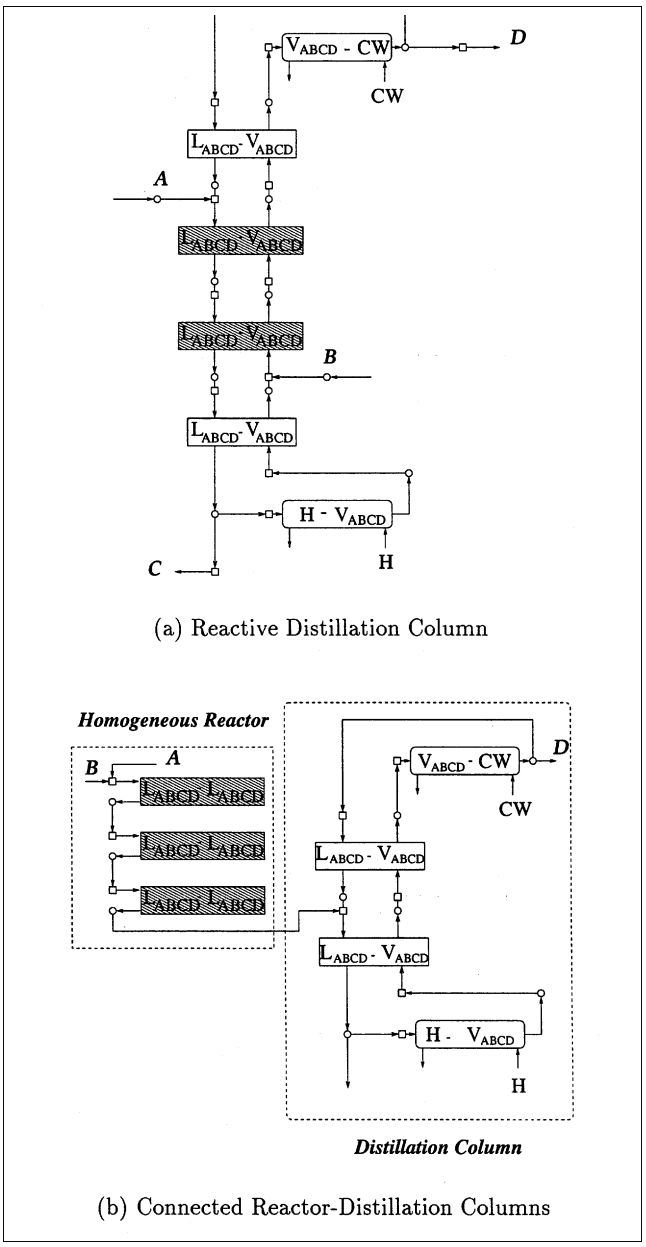

Figure 2. Possible process alternatives.

Driving Force Constraints

Mathematical foundations

Within a mass-/heat-transfer module, mass transfer will take place between two participating streams of differing *potential*; that is, when two streams of different phase are not at equilibrium, and between reagent/product streams when reactions are possible. Feasible mass transfer between streams is ensured by imposing a set of "driving force constraints" based on Gibbs free energy, the form of which is dependent on the type of stream match and phenomena taking place.

Consider a Liquid-Vapor mass/heat exchange block for a multicomponent system where in general, mass transfer between the streams can occur due to separation and reactive phenomena. At constant temperature and pressure (taking the module to be a closed system), mass transfer will occur when the total Gibbs free energy $(nG)^{\text{tot}}$ of the system decreases, that is

$$d(nG)^{\text{tot}}_{T,P} \le 0 \tag{2}$$

When the number of moles of component i in the liquid stream of the system decreases ($dn_i^L \le 0$), either due to consumption in reaction and/or mass transfer from the liquid to the vapor phase

$$f^{LI}x_i^{LI} - f^{LO}x_i^{LO} \ge 0 \tag{3}$$

It follows from Eq. 2 that

$$\left[\frac{\partial(nG)^{\text{tot}}}{\partial n_i^L}\right]_{T,P} \ge 0 \tag{4}$$

When the number of moles of component i in the liquid stream of the system increases, that is, $dn_i^L \ge 0$, it is trivial to see that the sign of the inequalities in Eqs. 3 and 4 are reversed. The conjecture is thus proposed that in general, mass transfer within the module due to separation and/or reaction is consistently limited by

$$\mathcal{G}1_i * \mathcal{G}2_i \ge 0 \qquad \forall i = 1, \ldots C \tag{5}$$

where we define

$$\mathcal{G}1_i = f^{LI}x_i^{LI} - f^{LO}x_i^{LO} \tag{6}$$

$$\mathcal{G}2_i = \left[\frac{\partial(nG)^{\text{tot}}}{\partial n_i^L}\right]_{T,P} \tag{7}$$

For liquid-vapor matches with no reaction, $\partial(nG)^{\text{tot}}/\partial n_i^L$ represents the distance from phase equilibrium, and as shown in earlier work (Ismail et al., 1997), feasible mass transfer is ensured by constraining the adjacent streams on both sides of the module. For liquid-vapor matches with reaction, mass transfer is constrained at the liquid outlet side of the module.

Consider a multicomponent liquid-vapor mixture with k reactions occurring in the liquid phase. Mass conservation for each component requires

$$n_i^L + n_i^V = n_i^0 + \sum_k \nu_{ik}\epsilon_k \tag{8}$$

where by convention the stoichiometric coefficient ν_{ik} for reaction r is positive for products, negative for reactants, and zero for inerts, and n_i^0 is the initial number of moles.

Differentiating

$$dn_i^L + dn_i^V = \sum_k \nu_{ik} d\epsilon_k$$

$$dn_i^V = -dn_i^L + \sum_k \nu_{ik} d\epsilon_k \tag{9}$$

The fundamental relation for the Gibbs free energy of the mixture is given by

$$d(nG)^{\text{tot}} = (nV)dP - (nS)dT + \sum_i \left(\mu_i^L dn_i^L + \mu_i^V dn_i^V\right) \tag{10}$$

At constant T and P

$$d(nG)^{\text{tot}} = \sum_i \left(\mu_i^L dn_i^L + \mu_i^V dn_i^V\right) \tag{11}$$

$$= \sum_i \mu_i^L dn_i^L + \sum_i \mu_i^V \left(-dn_i^L + \sum_k \nu_{ik} d\epsilon_k\right) \tag{12}$$

$$= \sum_i \left(\mu_i^L - \mu_i^V\right) dn_i^L + \sum_i \sum_k \nu_{ik}\mu_i^V d\epsilon_k \tag{13}$$

Approximating $\partial\mu_i/\partial n_i^L \approx 0$

$$\frac{\partial(nG)^{\text{tot}}}{\partial n_i^L} = \mu_i^L - \mu_i^V + \sum_i \sum_k \nu_{ik}\mu_i^V \frac{\partial\epsilon_k}{\partial n_i^L} \tag{14}$$

The chemical potential is given by

$$\mu_i^L = \Delta G_i^f + RT \ln\left(\gamma_i^L x_i^L P_i^{\text{sat},L}\right) \tag{15}$$

$$\mu_i^V = \Delta G_i^f + RT \ln\left(\phi_i^V x_i^V P_{\text{tot}}\right) \tag{16}$$

where ΔG_i^f is the standard Gibbs function of formation of i from its elements at T and 1 atm. Therefore

$$\frac{\partial(nG)^{\text{tot}}}{\partial n_i^L} = RT\left[\ln\left(\gamma_i^L x_i^L P_i^{\text{sat},L}\right) - \ln\left(\phi_i^V x_i^V P_{\text{tot}}\right)\right] + \sum_i \sum_k \nu_{ik}\left[\Delta G_i^f + RT \ln\left(\phi_i^V x_i^V P_{\text{tot}}\right)\right] \frac{\partial\epsilon_k}{\partial n_i^L} \tag{17}$$

It is the sign of this expression that is of interest, and thus we can divide through by the positive product RT to obtain the expression required for the constraint in Eq. 5

$$\mathcal{G}2_i = \ln\left[\frac{\gamma_i^L x_i^L P_i^{\text{sat},L}}{\phi_i^V x_i^V P_{\text{tot}}}\right] + \sum_i \sum_k \left[\frac{\nu_{ik}\Delta G_i^f}{RT} + \nu_{ik} \ln\left(\phi_i^V x_i^V P_{\text{tot}}\right)\right] \frac{\partial\epsilon_k}{\partial n_i^L} \tag{18}$$

Driving force constraints can be analogously derived for liquid-liquid matches with reaction (Rahim Ismail, 1998).

The driving force constraints have the following features:

- Reaction kinetics are utilized and the dimensionless term $(\partial\epsilon_k/\partial n_i^L)$ is system dependent and must be analytically derived.
- When no reaction occurs, the constraint for reactive liquid-vapor matches reduces to the form used for nonreactive liquid-vapor matches (pure separation).
- When simultaneous reaction and separation occur, mass transfer is constrained at the liquid outlet side of the module, as compared to the pure separation case where adjacent streams on both sides of the module are constrained.

• To reduce the nonlinear terms, the constraint in Eq. 5 can be recasted to a set of mixed integer constraints by the introduction of a set of binary variables to denote the mass-transfer direction of each component in a mass/heat transfer block (Ismail et al., 1999a).

Analysis

To illustrate the consistency of the derived driving force constraints for combined reaction-separation phenomena, we consider the simulation of one typical reactive distillation system, the production of MTBE. MTBE is produced by the catalytic reaction of isobutylene (IB) and methanol (MeOH) in the liquid phase using an ion-exchange resin (Rehfinger and Hoffmann, 1990) or sulfuric acid (Al-Jarallah et al., 1988). The reaction scheme is

$$\text{MeOH} + \text{IB} \rightleftharpoons \text{MTBE} \tag{19}$$

An important side reaction occurs when the isobutylene reacts with itself to form diisobutylene, but this can be eliminated by the selection of appropriate catalyst particles (Rehfinger and Hoffmann, 1990).

Reactive distillation is a commercially economically attractive method with which to produce MTBE, enabling high isobutylene conversion and high purity MTBE to be produced in a single unit. The nonreactive mixture of methanol, isobutylene, and MTBE is highly nonideal, exhibiting two binary minimum boiling azeotropes: one between methanol and isobutylene, one between methanol and MTBE. However, at chemical reaction equilibrium the reactive mixture exhibits no azeotropes due to the elimination of the distillation boundaries by reaction (Barbosa and Doherty, 1998d). The simultaneous decomposition of MTBE to methanol and isobutylene and conversion of methanol and isobutylene to MTBE avoids the existence of MeOH-MTBE or MeOH-IB binary azeotropic mixtures, allowing reaction equilibrium to be reached.

In this work we consider the ion-exchange resin catalyzed reaction (Amberlyst 15), where the intrinsic rate of MTBE formation as determined by Rehfinger and Hoffmann (1990) is

$$r = k\left[\frac{a_{\text{IB}}}{a_{\text{MeOH}}} - \frac{1}{Ka}\frac{a_{\text{MTBE}}}{a_{\text{MeOH}}^2}\right] \tag{20}$$

The reaction rate is related to the number of acid groups, such that r denotes rate per unit mass of dry catalyst resin. The reaction equilibrium constant Ka is directly proportional to an attainable conversion of reactant components and increases exponentially with decreasing temperature, as expected for an exothermic reaction. The expression proposed by Colombo et al. (1983) is utilized

$$\ln Ka = -10.0982 + \frac{4{,}254.05}{T} + 0.2667 \ln T \tag{21}$$

The reaction rate constant k is much less temperature dependent, is given by Rehfinger and Hoffmann (1990) and is the following (assuming an amount of acid groups on the Amberlyst 15 resin per unit mass equal to 4.9 equiv/kgr)

$$k = 8.5132 \times 10^{13} \exp\left[\frac{-11{,}113.78}{T}\right] \quad (\text{kmol/h} \cdot \text{kg cat}) \tag{22}$$

Table 1. MTBE Production: Thermodynamic Properties

	C1	C2	C3	ΔG^f, kJ/kmol
MeOH	23.49989	3643.31362	−33.434	-1.6242×10^5
IB4	20.64556	2125.74886	−33.16	5.8074×10^4
NB4	20.64917	2132.42000	−33.15	-1.6560×10^4
MTBE	20.71616	2571.5846	−48.406	-1.2544×10^5

$$\ln P^{\text{sat}} = C1 - \frac{C2}{C3 + T} \quad \text{(Pa, K)}$$

Uniquac equation

$$\ln\gamma_i = \ln\gamma_i^c + \ln\gamma_i^r$$

$$\ln\gamma_i^r = q_i\left[1 - \ln\left(\sum_j \theta_j\tau_{ji}\right) - \sum_k\left(\frac{\theta_k\tau_{ik}}{\sum_j\theta_j\tau_{jk}}\right)\right]$$

$$\ln\gamma_i^c = 1 - J_i + \ln J_i - 5q_i\left[1 - \frac{J_i}{Li} + \ln\left(\frac{J_i}{L_i}\right)\right]$$

$$J_i = \frac{r_i}{\sum_j r_j x_j} \qquad L_i = \frac{q_i}{\sum_j q_j x_j}$$

$$\tau_{ji} = \exp\left(\frac{-\ln t_{ji}}{RT}\right) \qquad \tau_{ii} = 1$$

Binary Interaction Parameters Int_{ij}, kcal/kmol

	Meoh	IB4	NB4	MTBE
Meoh	0.0	−70.003	−70.003	−174.94
IB4	1,403.5	0.0	0.0	103.73
NB4	1,403.5	0.0	0.0	103.73
MTBE	931.43	−48.931	−48.931	0.0

Relative Molecular Volume and Surface Areas

	Meoh	IB4	NB4	MTBE
r_i	1.4311	2.9195	2.9209	4.0693
q_i	1.432	2.684	2.564	3.556

The reaction mixture is a strongly nonideal liquid and the UNIQUAC equation is utilized to calculate the liquid activity coefficients, as given in Table 1 with the Antoine coefficients.

The production of MTBE in a reactive column as simulated by Jacobs and Krishna (1993) and Hauan et al. (1995) is reproduced using AspenPlus. Of interest is a set of five equilibrium trays in the reactive zone of the column, which is simulated with fixed liquid inlet to the top tray and vapor inlet to the bottom tray (Table 2). The composition profiles obtained are shown in Figures 3 and 4, highlighting some of the peculiarities which make reactive distillation feasible for MTBE production. On all the trays, MTBE is generated by reaction 19 giving a total generation of 111.78 kmol/h, with the reaction rate increasing down the trays with the temperature. In terms of boiling point, the order of volatility of the pure components are (from lightest to heaviest) IB (+NB4) > MTBE > MeOH, thus one would expect MeOH to be shifted towards the bottom tray, and IB towards the top tray. As shown in Figure 3, the composition profile of the unreacted methanol initially decreases, then increases up the trays, featuring a switch in its mass-transfer direction. This is due to the existence of the minimum boiling nonreactive binary azeotrope between the inert n-butene and methanol, which

Table 2. MTBE Simulation

Specifications	Liquid Inlet	Vapor Inlet
Temp. (K)	348.79	355.413
Flow rate (kmol/h)	9611.64	9,865.51
X_{MeOH}	0.02262	0.04434
X_{IB}	0.00184	0.04074
X_{NB4}	0.97344	0.86971
X_{MTBE}	0.00209	0.04521
Pressure: 11 atm		
Catalyst mass: 300 kg per tray		

$\mathcal{G}1 * \mathcal{G}2$ *Values* Tray No.	Methanol	Isobutene	*n*-butene	MTBE
1	73.97371681	312.62260194	43.90351270	1232.90237762
2	110.53589518	283.19826454	8.02517744	361.06933612
3	4.40159917	229.07033453	1.94048716	149.99958523
4	69.12648927	177.61180879	0.42641232	73.55549641
5	60.49890977	146.74944437	0.04870678	33.38083490

tends to shift the methanol up the trays. In the complete column, this eventually results in the heaviest component featuring in the distillate. The other minimum boiling azeotrope between methanol and MTBE also aids the upward movement of methanol in the column, resulting in more methanol being reacted away, and resulting in the MTBE composition profile to increase down the trays. The composition profile of isobutylene decreases up the trays as it becomes depleted

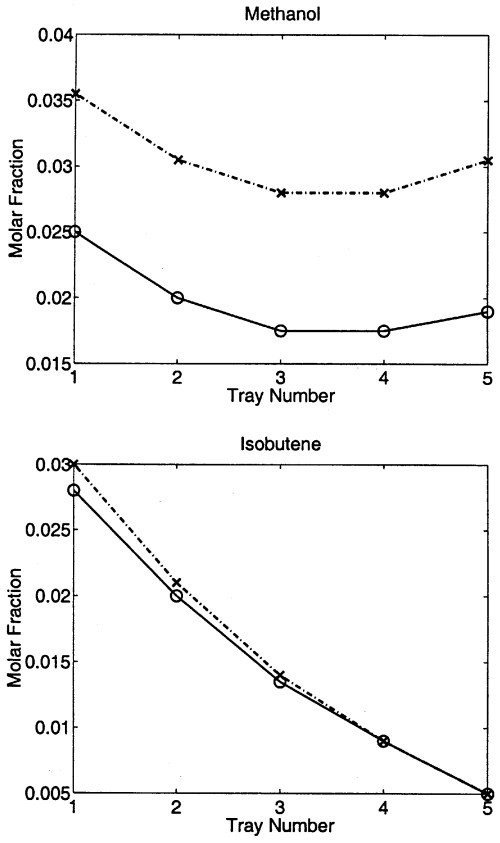

Figure 3. (Part A) MTBE simulation: composition profiles.

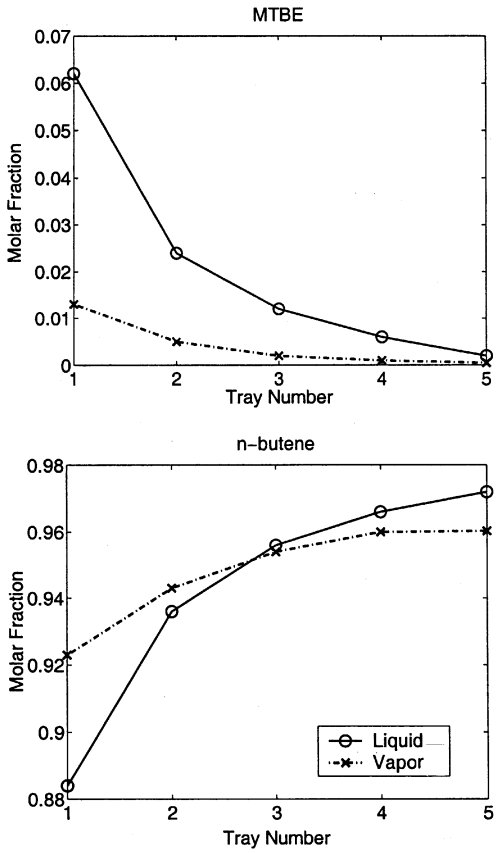

Figure 4. (Part B) MTBE simulation: composition profiles.

through reaction, while that of the inert increases due to its high volatility. Although affecting the behavior of the system, the nonreactive azeotropes are "reacted" away and do not appear.

Based on the given reaction rate, expressions for $\partial\epsilon/\partial n_i^L$ can be derived for use in the driving force constraints to give (Appendix A)

$$\frac{\partial\epsilon}{\partial n_{\mathrm{IB}}^L} = \left[\frac{\gamma_{\mathrm{IB}}}{\gamma_{\mathrm{MeOH}}x_{\mathrm{MeOH}}} + \frac{\gamma_{\mathrm{IB}}x_{\mathrm{IB}}}{\gamma_{\mathrm{MeOH}}x_{\mathrm{MeOH}}} - \frac{2}{Ka}\frac{\gamma_{\mathrm{MTBE}}x_{\mathrm{MTBE}}}{\gamma_{\mathrm{MeOH}}^2 x_{\mathrm{MeOH}}^2}\right]\left(\frac{kM_{\mathrm{cat}}}{f}\right) \tag{23}$$

$$\frac{\partial\epsilon}{\partial n_{\mathrm{MeOH}}^L} = \left[\frac{\gamma_{\mathrm{IB}}x_{\mathrm{IB}}}{\gamma_{\mathrm{MeOH}}x_{\mathrm{MeOH}}^2}(x_{\mathrm{MeOH}}-1) - \frac{2}{Ka}\frac{\gamma_{\mathrm{MTBE}}x_{\mathrm{MTBE}}}{\gamma_{\mathrm{MeOH}}^2 x_{\mathrm{MeOH}}^3}(x_{\mathrm{MeOH}}-1)\right]\left(\frac{kM_{\mathrm{cat}}}{f}\right) \tag{24}$$

$$\frac{\partial\epsilon}{\partial n_{\mathrm{MTBE}}^L} = -\left[\frac{1}{Ka}\frac{\gamma_{\mathrm{MTBE}}}{\gamma_{\mathrm{MeOH}}^2 x_{\mathrm{MeOH}}^2}(2x_{\mathrm{MTBE}}+1)\right]\left(\frac{kM_{\mathrm{cat}}}{f}\right) \tag{25}$$

$$\frac{\partial\epsilon}{\partial n_{\mathrm{NB4}}^L} = 0 \tag{26}$$

The driving force constraints are evaluated on every tray and as shown in Table 2, they are consistent with the equilibrium model with $\mathcal{G}1 * \mathcal{G}2 \geq 0$, able to capture the complex effects between separation and reaction.

Synthesis Framework

Based on the mass-/heat-transfer modular representation described earlier, and the driving force constraints described in the previous section, a systematic framework is proposed in this section which includes the following detailed features.

Stream superset

A stream superset is constructed to account for all possible initial, intermediate, and final streams that may exist in a process. In this framework a stream is defined by its phase. Therefore, in the case of a general mixed stream containing all components concerned, all the possible phases of this stream must be considered. Consider the synthesis example given earlier. Given that the mixture *ABCD* is homogeneous in the range of operating conditions considered, all possible streams can be represented as instances of a liquid stream, a vapor stream, a hot utility stream and a cold utility stream

$$L_{\mathrm{ABCD}}, V_{\mathrm{ABCD}}, St, CW$$

Mass-/heat-exchange matches

Mass-/Heat-Exchange Possibilities. Stream matches are considered between streams where mass and/or heat transfer can occur. For reactive/separation systems with reaction in the liquid phase, three types of matches are possible:

(1) *Liquid-liquid matches*

Mass transfer between two liquid streams is possible, whereby a component is transferred from one stream to another due to consumption or generation. For example, a liquid stream rich in reactants *A* and *B* will tend to give away or transfer *C* to a liquid product stream. Such a match would represent a reactor module.

(2) *Liquid-vapor matches without reaction*

Mass transfer between a liquid stream and vapor stream is possible due to volatility differences, representing a pure separator module, such as an aggregate of distillation trays.

(3) *Liquid-vapor matches with reaction*

Simultaneous mass transfer due to volatility differences and reaction results in such a match, representing a reactor/separator module, for example, an aggregate of reactive distillation columns.

To account for multiple mass exchange patterns that exist in multicomponent systems, multiple exchangers for each match are considered. The appropriate driving force constraints are introduced in each mass/heat exchange module to determine the mass-transfer direction of a component within the block and ensure feasibility of reaction and phase change. A summary of the constraints, as derived for liquid-vapor with reactions in the previous section, is given in Table 3.

Pure Heat Exchange Possibilities. To simplify the problem, only heat transfer between process and utility streams is considered, that is, no heat integration between process streams. For the synthesis problem in the Problem Statement section heat exchange matches are thus possible between each of the utility streams (St, CW) and the process streams (L_{ABCD}, V_{ABCD}). Feasibility of heat transfer is ensured by a minimum positive temperature difference between the hot and cold streams at the inlet and outlet of the exchanger. When phase change occurs in heat exchangers, the transferred heat includes vaporization/condensation enthalpy.

Mass/heat exchange superstructure

Block-superstructure rules are employed to develop a mass/heat exchange superstructure based on the postulated stream matches. For simplification purposes in this work, no stream heat integration is considered and the mass/heat exchanger is connected to two utility exchangers, a heater and a cooler. The building blocks of the network superstructure are (see Figure 5) initial stream splitters for each possible initial (feed) stream, final stream mixers for each possible product

Table 3. Driving Force Constraints

(1) Liquid-Vapor Match: Pure Separation

$$\mathcal{G}1_i = f^{LI}x_i^{LI} - f^{LO}x_i^{LO}$$
$$\mathcal{G}2_i = \gamma_i^{LO}x_i^{LO}P_i^{\mathrm{sat},LO} - \phi_i^{VI}x_i^{VI}P_{\mathrm{tot}}$$
$$\mathcal{G}3_i = \gamma_i^{LI}x_i^{LI}P_i^{\mathrm{sat},LI} - \phi_i^{VO}x_i^{VO}P_{\mathrm{tot}}$$

$\mathcal{G}1_i\mathcal{G}2_i \geq 0$
$\mathcal{G}1_i\mathcal{G}3_i \geq 0$

(2) Liquid-Vapor Match: Reaction and Separation

$$\mathcal{G}1_i = f^{LI}x_i^{LI} - f^{LO}x_i^{LO}$$
$$\mathcal{G}2_i = \ln\left(\frac{\gamma_i^{LO}x_i^{LO}P_i^{\mathrm{sat},LO}}{\phi_i^{VI}x_i^{VI}P_{\mathrm{tot}}}\right) + \sum_j\sum_k\left[\frac{\nu_{jk}\Delta G_j^f}{RT^{LO}} + \nu_{jk}\ln(\phi_j^{VI}x_j^{VI}P_{tot})\right]\frac{\partial\epsilon_k}{\partial n_i^L}$$

$\mathcal{G}1_i\mathcal{G}2_i \geq 0$

(3) Liquid-Liquid Match: Pure Reaction

$$\mathcal{G}1_i = f^{LI}x_i^{LI} - f^{LO}x_i^{LO}$$
$$\mathcal{G}2_i^{L1-L2} = \sum_i\sum_k \nu i_k\left[\frac{\Delta G_i^f}{RT^{LO}} + \ln(\gamma_i^{LO}x_i^{LO}P_i^{\mathrm{sat},LO})\right]\frac{\partial\epsilon_k}{\partial n_i^L}$$

$\mathcal{G}1_i\mathcal{G}2_i \geq 0$

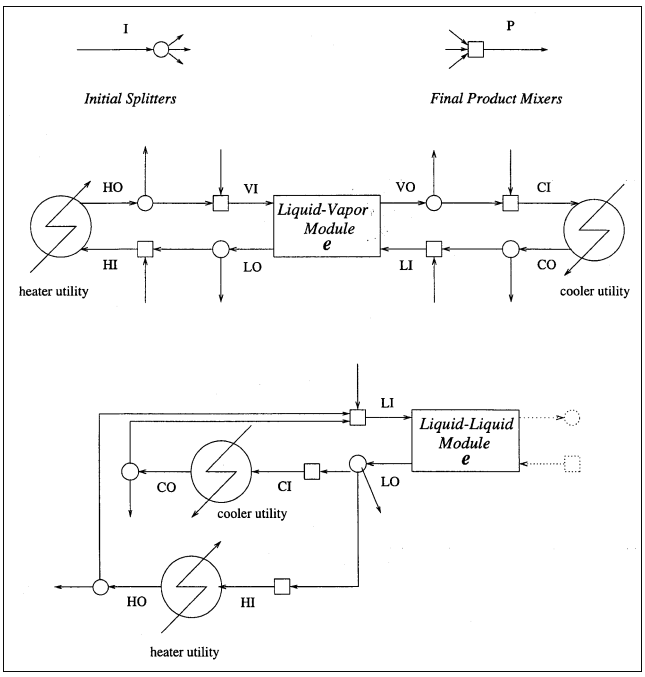

Figure 5. Superstructure building blocks.

stream, and mass/heat exchange modules with connected heat exchange modules.

All possible interconnections between the splitters and the mixers of the above blocks are defined with the assumption that only streams of the same phase can be mixed. For instance, flows from initial splitters are directed to the mixers of mass/heat and heat exchange modules and final mixers of product streams.

Mathematical Model

We introduce the following sets for the streams of the mass/heat exchange superstructure:

$I = \{n/n$ initial stream$\}$
$P = \{p/p$ product stream$\}$
$LI_e = \{s/s$ liquid inlet stream li in mass/heat exchanger $e\}$
$LO_e = \{s/s$ liquid inlet stream lo in exchanger $e\}$
$VI_e = \{s/s$ vapor inlet stream vi in mass/heat exchanger $e\}$
$VO_e = \{s/s$ vapor outlet stream vo in exchanger $e\}$
$HI_e = \{s/s$ inlet stream hi of the utility heater of module $e\}$
$HO_e = \{s/s$ outlet stream ho of the utility heater of module $e\}$
$CI_e = \{s/s$ inlet stream ci of the utility cooler of module $e\}$
$CO_e = \{s/s$ outlet stream co of the utility cooler of module $e\}$
$LL_{ee'} = \{s/s$ interconnecting stream from liquid outlet splitter of module e to liquid inlet mixer of module $e'\}$
$LH_{ee'} = \{s/s$ interconnecting stream from liquid outlet splitter of module e to utility heater of module $e'\}$
$LC_{ee'} = \{s/s$ interconnecting stream from liquid outlet splitter of module e to utility cooler of module $e'\}$
$LP_{ep} = \{s/s$ interconnecting stream from liquid outlet splitter of module e to final mixer of liquid product $p\}$
$VV_{ee'} = \{s/s$ interconnecting stream from vapor outlet splitter of module e to vapor inlet mixer of module $e'\}$
$VC_{ee'} = \{s/s$ interconnecting stream from vapor outlet splitter of module e to utility cooler of module $e'\}$
$VP_{ep} = \{s/s$ interconnecting stream from liquid outlet splitter of module e to final mixer of vapor product $p\}$
$IL_{ne} = \{s/s$ interconnecting stream from initial stream n to liquid inlet mixer of module $e\}$
$IV_{ne} = \{s/s$ interconnecting stream from initial stream n to vapor inlet mixer of module $e\}$
$IH_{ne} = \{s/s$ interconnecting stream from initial stream n to utility heater of module $e\}$
$IC_{ne} = \{s/s$ interconnecting stream from initial stream n to utility cooler of module $e\}$
$IP_{np} = \{s/s$ interconnecting stream from initial stream n to final mixer of product $p\}$
$HL_{ee'} = \{s/s$ interconnecting stream from utility heater of module e to liquid inlet mixer of module $e'\}$
$HV_{ee'} = \{s/s$ interconnecting stream from utility heater of module e to vapor inlet mixer of module $e'\}$
$HP_{ep} = \{s/s$ interconnecting stream from utility heater of module e to final mixer of product $p\}$
$CL_{ee'} = \{s/s$ interconnecting stream from utility cooler of module e to liquid inlet mixer of module $e'\}$
$CP_{ep} = \{s/s$ interconnecting stream from utility cooler of module e to final mixer of product $p\}$

In general, the initial streams and product streams can be liquid or vapor phase and thus we have

$$I = N^{\text{liq}} \cup N^{\text{vap}}$$

$$P = P^{\text{liq}} \cup P^{\text{vap}}$$

where
N^{liq} = set of liquid phase initial streams
N^{vap} = set of vapor phase initial streams
P^{liq} = set of liquid phase products
P^{vap} = set of vapor phase products

A set of E modules are considered

$$E = E^{\text{sep}} \cup E^{\text{resep}} \cup E^{\text{reac}}$$

where
E^{sep} = set of liquid-vapor separation modules
E^{resep} = set of liquid-vapor separation/reaction modules
E^{reac} = set of liquid-liquid reaction modules

Binary variables are introduced to denote

- the existence (or not) of each module

$$y_e = \begin{cases} 1 & \text{if module } e \text{ exists} \\ 0, & \text{otherwise} \end{cases}$$

- the mass-transfer direction of each component in each module.

$$yt_{ei} = \begin{cases} 1, & \text{if component } i \text{ in module } e \text{ is transferred from liquid to vapor and/or consumed in reaction} \\ 0, & \text{if component } i \text{ in module } e \text{ is transferred from vapor to liquid and/or produced by reaction} \end{cases}$$

- the existence (or not) of superstructure streams in the final flowsheet as described in Table 4 (interconnecting

Table 4. Structural Variables

Variable	Denoting the Existence of:
yh_e	Utility heater of module e
yc_e	Utility cooler of module e
$yll_{ee'}$	Interconnecting stream from liquid outlet splitter of module e to liquid inlet mixer of module e'
$ylh_{ee'}$	Liquid stream from liquid outlet splitter of module e to utility heater of module e'
$ylc_{ee'}$	Liquid stream from liquid outlet splitter of module e to utility cooler of module e'
ylp_{ep}	Interconnecting stream from liquid outlet splitter of module e to the final mixer of liquid product stream p
$yvv_{ee'}$	Interconnecting stream from vapor outlet splitter of module e to vapor inlet mixer of module e'
$yvc_{ee'}$	Vapor stream from vapor outlet splitter of module e to utility cooler of module e'
yvp_{ep}	Interconnecting stream from vapor outlet splitter of module e to the final mixer of vapor product stream p
yIl_{ne}	Interconnecting stream from initial stream n to liquid inlet mixer of module e
yIv_{ne}	Interconnecting stream from initial stream n to vapor inlet mixer of module e
yIh_{ne}	Interconnecting stream from initial stream n to utility heater of module e
yIc_{ne}	Interconnecting stream from initial stream n to utility cooler of module e
yIp_{np}	Interconnecting stream from initial stream n to final mixer of product stream p
$yhl_{ee'}$	Liquid stream from utility heater of module e to liquid inlet mixer of module e'
$yhv_{ee'}$	Vapor stream from utility heater of module e to vapor inlet mixer of module e'
yhp_{ep}	Interconnecting stream from utility heater of module e to the final mixer of product stream p
$ycl_{ee'}$	Interconnecting stream from utility cooler of module e to liquid inlet mixer of module e'
ycp_{ep}	Interconnecting stream from utility cooler of module e to the final mixer of product stream p

streams between the splitters and mixers). As these variables are not necessary, their presence does not increase the combinatorial complexity of the synthesis problem. They are utilized to simplify the solution of the nonlinear part of the superstructure model and to facilitate the introduction of logical constraints to the model (as detailed later).

The mass/heat exchange superstructure mathematical model then involves:

(A) Mass balance for total stream flows at

• initial stream splitters

$$f_n^I - \sum_e f_{ne}^{IL} - \sum_e f_{ne}^{IH} - \sum_{e \in E^{\text{reac}}} f_{ne}^{IC} - \sum_{p \in P^{\text{liq}}} f_{np}^{IP} = 0 \quad \forall n \in N^{\text{liq}} \tag{27}$$

$$f_n^I - \sum_e f_{ne}^{IV} - \sum_e f_{ne}^{IC} - \sum_{p \in P^{\text{vap}}} f_{np}^{IP} = 0 \quad \forall n \in N^{\text{vap}} \tag{28}$$

• splitters at the outlets of each side of module e

$$f_e^{LO} - \sum_{e'} \left(f_{ee'}^{LL} + f_{ee'}^{LH} \right) - \sum_{e' \in E^{\text{reac}}} f_{ee'}^{LC} - \sum_{p \in P^{\text{liq}}} f_{ep}^{LP} = 0 \tag{29}$$

$$f_e^{VO} - \sum_{e'} \left(f_{ee'}^{VV} + f_{ee'}^{VC} \right) - \sum_{p \in P^{\text{vap}}} f_{ep}^{VP} = 0 \tag{30}$$

$$f_e^H - \sum_{e'} f_{ee'}^{HV} - \sum_{p \in P^{\text{vap}}} f_{ep}^{HP} = 0 \quad \forall e \in \left(E^{\text{sep}} \cup E^{\text{resep}} \right) \tag{31}$$

$$f_e^H - \sum_{e'} f_{ee'}^{HL} - \sum_{p \in P^{\text{liq}}} f_{ep}^{HP} = 0 \quad \forall e \in E^{\text{reac}} \tag{32}$$

$$f_e^C - \sum_{e'} f_{ee'}^{CL} - \sum_{p \in P^{\text{liq}}} f_{ep}^{CP} = 0 \tag{33}$$

• mixers at the inlets of each side of module e

$$f_e^{LI} - \sum_{n \in N^{\text{liq}}} f_{ne}^{IL} - \sum_{e'} \left(f_{e'e}^{LL} + f_{e'e}^{CL} \right) - \sum_{e' \in E_{\text{reac}}} f_{e'e}^{HL} = 0 \tag{34}$$

$$f_e^{VI} - \sum_{n \in N^{\text{vap}}} f_{ne}^{IV} - \sum_{e'} \left(f_{e'e}^{VV} + f_{e'e}^{HV} \right) = 0 \tag{35}$$

$$f_e^C - \sum_{n \in N^{\text{vap}}} f_{ne}^{IC} - \sum_{e'} f_{e'e}^{VC} = 0 \quad \forall e \in \left(E^{\text{sep}} \cup E^{\text{resep}} \right) \tag{36}$$

$$f_e^C - \sum_{n \in N^{\text{liq}}} f_{ne}^{IC} - \sum_{e'} f_{e'e}^{LC} = 0 \quad \forall e \in E^{\text{reac}} \tag{37}$$

$$f_e^H - \sum_{n \in N^{\text{liq}}} f_{ne}^{IH} - \sum_{e'} f_{e'e}^{LH} = 0 \tag{38}$$

• final product mixers

$$f_p^P - \sum_{n \in N^{\text{liq}}} f_{np}^{IP} - \sum_e f_{ep}^{LP} - \sum_e f_{ep}^{CP} - \sum_{e \in E^{\text{reac}}} f_{ep}^{HP} = 0 \quad \forall p \in P^{\text{liq}} \tag{39}$$

$$f_p^P - \sum_{n \in N^{\text{vap}}} f_{np}^{IP} - \sum_e f_{ep}^{VP} - \sum_{e \in (E^{\text{sep}} \cup E^{\text{resep}})} f_{ep}^{HP} = 0 \quad \forall p \in P^{\text{vap}} \tag{40}$$

(B) Mass balances for each component at

• mixers prior to liquid and vapor sides and utility exchangers of each module e

$$f_e^{LI} x_{ei}^{LI} - \sum_{n \in N^{\text{liq}}} f_{ne}^{IL} x_{ni}^I - \sum_{e'} \left(f_{e'e}^{LL} x_{e'i}^{LO} + f_{e'e}^{CL} x_{e'i}^C \right) - \sum_{e' \in E^{\text{reac}}} f_{e'e}^{HL} x_{e'i}^H = 0 \tag{41}$$

$$f_e^{VI} x_{ei}^{VI} - \sum_{n \in N^{\text{vap}}} f_{ne}^{IV} x_{ni}^I - \sum_{e'} \left(f_{e'e}^{VV} x_{e'i}^{VO} + f_{e'e}^{HV} x_{e'i}^H \right) = 0 \tag{42}$$

$$f_e^C x_{ei}^C - \sum_{n \in N^{\text{vap}}} f_{ne}^{IC} x_{ni}^I - \sum_{e'} f_{e'e}^{VC} x_{e'i}^{VO} = 0 \quad \forall e \in \left(E^{\text{sep}} \cup E^{\text{resep}} \right) \tag{43}$$

$$f_e^C x_{ei}^C - \sum_{n \in N^{\text{liq}}} f_{ne}^{IC} x_{ni}^I - \sum_{e'} f_{e'e}^{LC} x_{e'i}^{LO} = 0 \quad \forall e \in E^{\text{reac}} \tag{44}$$

$$f_e^H x_{ei}^H - \sum_{n \in N^{\text{liq}}} f_{ne}^{IH} x_{ni}^I - \sum_{e'} f_{e'e}^{LH} x_{e'i}^{LO} = 0 \tag{45}$$

• final mixer of each product stream

$$f^P x_i^P - \sum_{n \in N^{\text{liq}}} f_{np}^{IP} x_{ni}^I - \sum_e f_{ep}^{LP} x_{ei}^{LO} - \sum_e f_{ep}^{CP} x_{ei}^C - \sum_{e \in E^{\text{reac}}} f_{ep}^{HP} x_{ei}^H = 0 \quad p \in P^{\text{liq}} \quad (46)$$

$$f^P x_i^P - \sum_{n \in N^{\text{vap}}} f_{np}^{IP} x_{ni}^I - \sum_e f_{ep}^{VP} x_{ei}^{VO} - \sum_{e \in (E^{\text{sep}} \cup E^{\text{resep}})} f_{ep}^{HP} x_{ei}^H = 0 \quad p \in P^{\text{vap}} \quad (47)$$

• around each mass/heat exchange block

$$f_e^{LI} x_{ei}^{LI} + f_e^{VI} x_{ei}^{VI} - f_e^{LO} x_{ei}^{LO} - f_e^{VO} x_{ei}^{VO} + \sum_k \nu_{ik} * r_{ek} * V_e = 0 \quad (48)$$

(C) Energy balances at

• mixers prior to liquid and vapor sides and utility exchangers of each module e

$$f_e^{LI} h_e^{LI} - \sum_{n \in N^{\text{liq}}} f_{ne}^{IL} h_n^I - \sum_{e'} \left(f_{e'e}^{LL} h_{e'}^{LO} + f_{e'e}^{CL} h_{e'}^{CO} \right) - \sum_{e' \in E^{\text{reac}}} f_{e'e}^{HL} h_{e'}^{HO} = 0 \quad (49)$$

$$f_e^{VI} h_e^{VI} - \sum_{n \in N^{\text{vap}}} f_{ne}^{IL} h_n^I - \sum_{e'} \left(f_{e'e}^{VV} h_{e'}^{VO} + f_{e'e}^{HV} h_{e'}^{HO} \right) = 0 \quad (50)$$

$$f_e^{HI} h_e^{HI} - \sum_{n \in N^{\text{liq}}} f_{ne}^{IH} h_n^I - \sum_{e'} f_{e'e}^{LH} h_{e'}^{LO} = 0 \quad (51)$$

$$f_e^{CI} h_e^{CI} - \sum_{n \in N^{\text{vap}}} f_{ne}^{IC} h_n^I - \sum_{e'} f_{e'e}^{VC} h_{e'}^{VO} = 0 \quad \forall e \in (E^{\text{sep}} \cup E^{\text{resep}}) \quad (52)$$

$$f_e^{CI} h_e^{CI} - \sum_{n \in N^{\text{liq}}} f_{ne}^{IC} h_n^I - \sum_{e'} f_{e'e}^{LC} h_{e'}^{LO} = 0 \quad \forall e \in E^{\text{reac}} \quad (53)$$

• around utility exchangers of each module e

$$Qh_e - f_e^H \left(h_e^{HO} - h_e^{HI} \right) = 0 \quad (54)$$

$$Qc_e - f_e^C \left(h_e^{CO} - h_e^{CI} \right) = 0 \quad (55)$$

• around each mass/heat exchange block e

$$f_e^{LI} h_e^{LI} + f_e^{VI} h_e^{VI} - f_e^{LO} h_e^{LO} - f_e^{VO} h_e^{VO} - \sum_k r_{ek} * V_e * \Delta H_{\text{reac},k} = 0 \quad (56)$$

where $\Delta H_{\text{reac},k}$ is the heat of reaction k

• final mixers of each product stream

$$f^P h^P - \sum_{n \in N^{\text{liq}}} f_{np}^{IP} h_n^I - \sum_e f_{ep}^{LP} h_e^{LO} - \sum_e f_{ep}^{CP} h_e^{CO} = 0 \quad p \in P^{\text{liq}} \quad (57)$$

$$f^P h^P - \sum_{n \in N^{\text{vap}}} f_{np}^{IP} h_n^I - \sum_e f_{ep}^{VP} h_e^{VO} - \sum_e f_{ep}^{HP} h_e^{HO} = 0 \quad p \in P^{\text{vap}} \quad (58)$$

(D) Summation of molar fractions

• for superstructure streams $s = LI, LO, VI, VO, C, H, P$

$$\sum_i x_{ei}^s - 1 = 0 \quad (59)$$

(E) Phase defining constraints

for liquid streams: $$\sum_i \left(\gamma_{ei}^s P_{ei}^{\text{sat},s} x_{ei}^s \right) / \left(\phi_{ei}^s P_{\text{tot}} \right) \le 1 \quad (60)$$

for vapor streams: $$\sum_i \left(x_{ei}^s \phi_{ei}^s P_{\text{tot}} \right) / \left(\gamma_{ei}^s P_{ei}^{\text{sat},s} \right) \le 1 \quad (61)$$

A lower bound may be enforced on these constraints to limit the level of superheating and supercooling, and/or to aid the solution procedure of the model. A value of 0.8 is utilized as a first guess in this work. When this bound is active, the value is relaxed.

(F) Mass-transfer driving force constraints for each component

The derived driving force constraints of the form (Eq. 5)

$$\mathfrak{G}1_{ei} * \mathfrak{G}2_{ei} \ge 0 \quad (62)$$

are rewritten as follows

$$(y_e + yt_{ei} - 2)\mathfrak{U} \le \mathfrak{G}1_{ei} \le (yt_{ei} + 1 - y_e)\mathfrak{U} \quad (63)$$

$$(y_e + yt_{ei} - 2)\mathfrak{U} \le \mathfrak{G}2_{ei} \le (yt_{ei} + 1 - y_e)\mathfrak{U} \quad (64)$$

where $\mathfrak{U}$ is a (large) positive number.

Note that in an existing module, that is, $y_e = 1$, Eqs. 63–64 become

$$(yt_{ei} - 1)\mathfrak{U} \le \mathfrak{G}1_{ei} \le yt_{ei}\mathfrak{U}$$

$$(yt_{ei} - 1)\mathfrak{U} \le \mathfrak{G}2_{ei} \le yt_{ei}\mathfrak{U}$$

Thus, when a component A is transferred from the liquid to vapor stream and/or consumed in reaction, that is, $yt_A = 1$

$$\left.\begin{array}{l} 0 \le \mathfrak{G}1_A \le \mathfrak{U} \\ 0 \le \mathfrak{G}2_A \le \mathfrak{U} \end{array}\right\} \Rightarrow \left.\begin{array}{l} \mathfrak{G}1_A \ge 0 \\ \mathfrak{G}2_A \ge 0 \end{array}\right.$$

Similarly, when $yt_A = 0$

$$\left.\begin{array}{l} -\mathfrak{U} \le \mathfrak{G}1_A \le 0 \\ -\mathfrak{U} \le \mathfrak{G}2_A \le 0 \end{array}\right\} \Rightarrow \left.\begin{array}{l} \mathfrak{G}1_A \le 0 \\ \mathfrak{G}2_A \le 0 \end{array}\right.$$

In either case, Eqs. 63–64 are consistent with Eq. 62.

In a nonexisting module, the driving forces are made redundant by imposing

$$yt_{ei} + y_e \ge 1 \quad (65)$$

When $y_e = 0$, this forces $yt_{ei} = 1$ such that Eqs. 63–64 are redundant, that is,

$$-\mathfrak{U} \le \mathfrak{G}1_{ei} \le 2\mathfrak{U}$$
$$-\mathfrak{U} \le \mathfrak{G}2_{ei} \le 2\mathfrak{U}$$

The driving force constraints for each type of mass/heat transfer module (as given in Table 3) are thus linearized to

For $e \in E^{sep}$

$$(y_e + yt_{ei} - 2)\mathfrak{U} \le f_e^{LI} x_{ei}^{LI} - f_e^{LO} x_{ei}^{LO} \le (yt_{ei} + 1 - y_e)\mathfrak{U} \quad (66)$$

$$(y_e + yt_{ei} - 2)\mathfrak{U} \le \gamma_{ei}^{LI} P_{ei}^{\mathrm{sat},LI} x_{ei}^{LI} - x_{ei}^{VO} P_{\mathrm{tot}} \le (yt_{ei} + 1 - y_e)\mathfrak{U} \quad (67)$$

$$(y_e + yt_{ei} - 2)\mathfrak{U} \le \gamma_{ei}^{LO} P^{\mathrm{sat},LO} x_{ei}^{LO} - x_{ei}^{VI} P_{\mathrm{tot}} \le (yt_{ei} + 1 - y_e)\mathfrak{U} \quad (68)$$

For $e \in E^{\mathrm{resep}}$

$$(y_e + yt_{ei} - 2)\mathfrak{U} \le f_e^{LI} x_{ei}^{LI} - f_e^{LO} x_{ei}^{LO} \le (yt_{ei} + 1 - y_e)\mathfrak{U} \quad (69)$$

$$(y_e + yt_{ei} - 2)\mathfrak{U} \le \mathfrak{G}2_{ei} \le (yt_{ei} + 1 - y_e)\mathfrak{U} \quad (70)$$

$$\mathfrak{G}2_{ei} = \ln\left[\frac{\gamma_{ei}^{LO} x_{ei}^{LO} P_{ei}^{\mathrm{sat},LO}}{\phi_{ei}^{VI} x_{ei}^{VI} P_{\mathrm{tot}}}\right] + \sum_i \sum_k \left[\frac{\nu_{ik} \Delta G_i^f}{RT_e^{LO}} + \nu_{ik} \ln\left(\phi_{ei}^{VI} x_{ei}^{VI} P_{\mathrm{tot}}\right)\right] \frac{\partial \epsilon_k}{\partial n_{ei}^L} \quad (71)$$

For $e \in E^{\mathrm{reac}}$

$$(y_e + yt_{ei} - 2)\mathfrak{U} \le f_e^{LI} x_{ei}^{LI} - f_e^{LO} x_{ei}^{LO} \le (yt_{ei} + 1 - y_e)\mathfrak{U} \quad (72)$$

$$(y_e + yt_{ei} - 2)\mathfrak{U} \le \mathfrak{G}2_{ei} \le (yt_{ei} + 1 - y_e)\mathfrak{U} \quad (73)$$

$$\mathfrak{G}2_{ei} = \sum_i \sum_k \nu_{ik} \left[\frac{\Delta G_i^f}{RT_e^{LO}} + \ln\left(\gamma_{ei}^{LO} x_{ei}^{LO} P_{ei}^{\mathrm{sat},LO}\right)\right] \frac{\partial \epsilon_k}{\partial n_{ei}^L} \quad (74)$$

where $\partial\epsilon/\partial n_{ei}^L$ (derived as illustrated in Appendix A) is calculated at conditions of the liquid outlet of each module e.

(G) Thermodynamic property calculation

- Reaction rate

$$r_{ek} = f\left(x_{ei}^{\mathrm{LO}}, T_e^{\mathrm{LO}}\right) \quad (75)$$

- Density

$$\rho_{m_e}^{\mathrm{LO}} = f\left(x_{ei}^{\mathrm{LO}}, T_e^{\mathrm{LO}}\right) \quad (76)$$

and the mixture density is given by

$$\frac{1}{\rho_{m_e}} = \sum_i \frac{x_{ei}}{\rho_{ei}}$$

- Vapor pressure, enthalpy and activity coefficient for $s = LI, LO, VI, VO, HI, HO, CI, CO, P$

$$P_{ei}^{\mathrm{sat},s} = f(T_e^s) \quad (77)$$
$$h^s = f(x_{ei}^s, T_e^s) \quad (78)$$
$$\gamma_{ei}^s = f(x_{ei}^s, T_e^s, P_{\mathrm{tot}}) \quad (79)$$
$$\phi_{ei}^s = f(x_{ei}^s, T_e^s, P_{\mathrm{tot}}) \quad (80)$$

(H) Logical constraints

These constraints are imposed to ensure that when a module does not exist, no interconnecting flow to the module mixer, through the module, or from the module splitter, exists. Similarly, when a module does exist, they ensure that there is at least one interconnecting flow to its mixer, and away from its splitter.

- to define the existence of each module of each superstructure stream

$$\left[f_e^{LI} + f_e^{LO} + f_e^{VI} + f_e^{VO}\right] - y_e \mathfrak{F}^{\max} \le 0 \quad (81)$$
$$f_e^H - yh_e \mathfrak{F}^{\max} \le 0 \quad (82)$$
$$f_e^C - yc_e \mathfrak{F}^{\max} \le 0 \quad (83)$$
$$Qh_e - yh_e \mathfrak{Q}^{\max} \le 0 \quad (84)$$
$$Qc_e - yc_e \mathfrak{Q}^{\max} \le 0 \quad (85)$$

where $\mathfrak{F}^{\max}$ is an upper bound to stream flows and $\mathfrak{Q}^{\max}$ is an upper bound to heat flows.

- to define the existence of interconnecting streams for $s = LL, LH, LC, LP, VV, VC, VP, IL, IV, IH, IC, IP, HL, HV, HP, CL, CP$

$$f_{ee}^s - y_{ee}^s \mathfrak{F}^{\max} \le 0 \quad (86)$$

that is, for $s = LL$,

$$f_{ee}^{LL} - yll_{ee} \mathfrak{F}^{\max} \le 0$$

- to ensure that utility exchangers exist only if the module exists

$$yh_e - y_e \le 0 \quad (87)$$
$$yc_e - y_e \le 0 \quad (88)$$

- to ensure that if a module exists there will be an inlet flow

$$y_e - \left[\sum_{n \in N^{\mathrm{liq}}} yIl_{ne} + \sum_{e'} yll_{e'e} + \sum_{e'} ycl_{e'e} + \sum_{e' \in E^{\mathrm{reac}}} yhl_{e'e}\right] \le 0 \quad (89)$$

$$y_e - \left[\sum_{n \in N^{\mathrm{vap}}} yIv_{ne} + \sum_{e'} yvv_{e'e} + \sum_{e'} yhv_{e'e}\right] \le 0 \quad (90)$$

$$yh_e - \left[\sum_{n \in N^{\mathrm{liq}}} yIh_{ne} + \sum_{e'} ylh_{e'e}\right] \le 0 \quad (91)$$

$$yc_e - \left[\sum_{n \in N^{\mathrm{vap}}} yIc_{ne} + \sum_{e'} yvc_{e'e}\right] \le 0 \quad \forall e \in (E^{\mathrm{sep}} \cup E^{\mathrm{resep}}) \quad (92)$$

$$yc_e - \left[\sum_{n \in N^{\mathrm{liq}}} yIc_{ne} + \sum_{e'} ylc_{e'e}\right] \le 0 \quad \forall e \in E^{\mathrm{reac}} \tag{93}$$

• to ensure that if a module exists there will be an outlet flow

$$y_e - \left[\sum_{e'} yll_{ee'} + \sum_{e'} ylh_{ee'} + \sum_{e' \in E^{\mathrm{reac}}} ylc_{ee'} + \sum_{p \in P^{\mathrm{liq}}} ylp_{ep}\right] \le 0 \tag{94}$$

$$y_e - \left[\sum_{e'} yvv_{ee'} + \sum_{e'} yvc_{ee'} + \sum_{p \in P^{\mathrm{vap}}} yvp_{ep}\right] \le 0 \tag{95}$$

$$yh_e - \left[\sum_{e'} yhv_{ee'} + \sum_{p \in P^{\mathrm{vap}}} yhp_{ep}\right] \le 0 \quad \forall e \in (E^{\mathrm{sep}} \cup E^{\mathrm{resep}}) \tag{96}$$

$$yh_e - \left[\sum_{e'} yhl_{ee'} + \sum_{p \in P^{\mathrm{liq}}} yhp_{ep}\right] \le 0 \quad \forall e \in E^{\mathrm{reac}} \tag{97}$$

$$yc_e - \left[\sum_{e'} ycl_{ee'} + \sum_{p} ycp_{ep}\right] \le 0 \tag{98}$$

• to ensure at least one feed point per initial stream

$$1 - \left[\sum_{e} yIl_{ne} + \sum_{e} yIh_{ne} + \sum_{e \in E^{\mathrm{reac}}} yIc_{ne} + \sum_{p \in P^{\mathrm{liq}}} yIp_{np}\right] \le 0, \quad n \in N^{\mathrm{liq}} \tag{99}$$

$$1 - \left[\sum_{e} yIv_{ne} + \sum_{e} yIc_{ne} + \sum_{p \in P^{\mathrm{vap}}} yIp_{np}\right] \le 0, \quad n \in N^{\mathrm{vap}} \tag{100}$$

• to ensure at least one source per product

$$1 - \left[\sum_{n \in N^{\mathrm{liq}}} yIp_{np} + \sum_{e} ylp_{ep} + \sum_{e} ycp_{ep} + \sum_{e \in E^{\mathrm{reac}}} yhp_{ep}\right] \le 0, \quad p \in P^{\mathrm{liq}} \tag{101}$$

$$1 - \left[\sum_{n \in N^{\mathrm{vap}}} yIp_{np} + \sum_{e} yvp_{ep} + \sum_{e \in (E^{\mathrm{sep}} \cup E^{\mathrm{resep}})} yhp_{ep}\right] \le 0, \quad p \in P^{\mathrm{vap}} \tag{102}$$

• to constrain the number of streams allowed at existing mixers

$$\left[\sum_{n \in N^{\mathrm{liq}}} yIl_{ne} + \sum_{e'} yll_{e'e} + \sum_{e'} ycl_{e'e} + \sum_{e' \in E^{\mathrm{reac}}} yhl_{e'e}\right] - y_e Nmix^{\max} \le 0 \tag{103}$$

$$\left[\sum_{n \in N^{\mathrm{vap}}} yIv_{ne} + \sum_{e'} yvv_{e'e} + \sum_{e'} yhv_{e'e}\right] - y_e Nmix^{\max} \le 0 \tag{104}$$

$$\left[\sum_{n \in N^{\mathrm{liq}}} yIh_{ne} + \sum_{e'} ylh_{e'e}\right] - yh_e Nmix^{\max} \le 0 \tag{105}$$

$$\left[\sum_{n \in N^{\mathrm{vap}}} yIc_{ne} + \sum_{e'} yvc_{e'e}\right] - yc_e Nmix^{\max} \le 0 \quad \forall e \in (E^{\mathrm{sep}} \cup E^{\mathrm{resep}}) \tag{106}$$

$$\left[\sum_{n \in N^{\mathrm{liq}}} yIc_{ne} + \sum_{e'} ylc_{e'e}\right] - yc_e Nmix^{\max} \le 0 \quad \forall e \in E^{\mathrm{reac}} \tag{107}$$

• to constrain the number of splits allowed at existing splitters

$$\left[\sum_{e'} yll_{ee'} + \sum_{e'} ylh_{ee'} + \sum_{e' \in E^{\mathrm{reac}}} ylc_{ee'} + \sum_{p \in P^{\mathrm{liq}}} ylp_{ep}\right] - y_e Nsplit^{\max} \le 0 \tag{108}$$

$$\left[\sum_{e'} yvv_{ee'} + \sum_{e'} yvc_{ee'} + \sum_{p \in P^{\mathrm{vap}}} yvp_{ep}\right] - y_e Nsplit^{\max} \le 0 \tag{109}$$

$$\left[\sum_{e'} yhv_{ee'} + \sum_{p \in P^{\mathrm{vap}}} yhp_{ep}\right] - yh_e Nsplit^{\max} \le 0 \quad \forall e \in (E^{\mathrm{sep}} \cup E^{\mathrm{resep}}) \tag{110}$$

$$\left[\sum_{e'} yhl_{ee'} + \sum_{p \in P^{\mathrm{liq}}} yhp_{ep}\right] - yh_e Nsplit^{\max} \le 0 \quad \forall e \in E^{\mathrm{reac}} \tag{111}$$

$$\left[\sum_{e'} ycl_{ee'} + \sum_{p} ycp_{ep}\right] - yc_e Nsplit^{\max} \le 0 \tag{112}$$

• to constrain the number of splits allowed at initial splitters

$$\left[\sum_{e} yIl_{ne} + \sum_{e} yIh_{ne} + \sum_{e \in E^{\mathrm{reac}}} yIc_{ne} + \sum_{p \in P^{\mathrm{liq}}} yIp_{np}\right] - Nsplit^{\max} \le 0, \quad n \in N^{\mathrm{liq}} \tag{113}$$

$$\left[\sum_{e} yIv_{ne} + \sum_{e} yIc_{ne} + \sum_{p \in P^{\mathrm{vap}}} yIp_{np}\right] - Nsplit^{\max} \le 0, \quad n \in N^{\mathrm{vap}} \tag{114}$$

• to constrain the number of product sources

$$\left[\sum_{n \in N^{\mathrm{liq}}} yIp_{np} + \sum_{e} ylp_{ep} + \sum_{e} ycp_{ep} + \sum_{e \in E^{\mathrm{reac}}} yhp_{ep}\right] - Nmix^{\max} \le 0, \quad p \in P^{\mathrm{liq}} \tag{115}$$

$$\left[\sum_{n \in N^{\mathrm{vap}}} yIp_{np} + \sum_{e} yvp_{ep} + \sum_{e \in (E^{\mathrm{sep}} \cup E^{\mathrm{resep}})} yhp_{ep}\right] - Nmix^{\max} \le 0, \quad p \in P^{\mathrm{vap}} \tag{116}$$

• nonredundancy constraints

$$y_{e+1} - y_e \le 0 \quad e \in E^{\mathrm{sep}} \tag{117}$$

$$y_{e+1} - y_e \le 0 \quad e \in E^{\mathrm{resep}} \tag{118}$$

$$y_{e+1} - y_e \le 0 \quad e \in E^{\mathrm{reac}} \tag{119}$$

Bounding the maximum number of stream splits and stream mixers allowed at splitters and mixers constrains the problem, aiding the solution. $Nmix^{\max} = Nsplit^{\max} = 5$ is utilized and is relaxed when the constraint is active.

Note that Eqs. 103–112 ensure that interconnecting streams only exist if the corresponding modules exist.

For example, when a module $e = 1$ does not exist $y_1 = 0$ and by Eqs. 87–88, its heater and cooler also do not exist $yh_1 = yc_1 = 0$. Equations 103–107 then ensure that none of the interconnecting streams to the mixers of module y_1 exist, forcing $yIl_{n1} = yll_{e1} = ycl_{e1} = yhl_{e1} = yIv_{n1} = yvv_{e1} = yhv_{e1} = yIh_{e1} = ylh_{e1} = yIc_{n1} = yvc_{e1} = ylc_{e1} = 0$. Similarly, Eqs. 108–112 ensure that none of the interconnecting streams from the splitters of module y_1 exist, forcing $yll_{1e} = ylh_{1e} = ylc_{1e} = ylp_{1p} = yvv_{1e} = yvc_{1e} = yvp_{1p} = yhv_{1e} = yhp_{1p} = yhl_{1e} = ycl_{1e} = ycp_{1p} = 0$.

(I) Objective Function

The objective function includes the cost of feeds, heat utilities and a module cost

$$Z = \sum_n C_n * f_n^I + \sum_e C_{cw} * Qc_e + \sum_e C_{\text{steam}} * Qh_e + \sum_e \text{Cost}_e * y_e \quad (120)$$

where C_{cw}, C_{steam} is the cold and heat utility cost and C_n is the feed (raw material) cost.

Since capital costing correlations cannot be directly applied (no prepostulation of process units), a pseudo-capital module cost Cost_e is introduced to penalize the number of modules selected in the final synthesis configuration. This may be a fixed cost or a function of the stream flows and holdup to account for the size and capacity of the module. To derive the form and coefficients of the latter function, Guthrie's costing correlation for a pressure vessel can be utilized as a base. While modeling, the module as a pressure vessel may not always be realistic, it can implicitly account for the size of the module and is utilized here to approximate the module cost as a function of its flow rate and holdup. Once synthesis alternatives are generated, detailed unit operation cost correlations can then be utilized if required. As derived in Appendix B, Cost_e is given by

$$\text{Cost}_e(\$) = 99.507\left(\frac{MW_e^{VI}}{\rho_e^{VI}}\right)^{0.25}\sqrt{f_e^{VI}}H^{0.802}(2.18 + F_c), \quad e \in (E^{\text{sep}} \cup E^{\text{resep}}) \quad (121)$$

$$\text{Cost}_e(\$) = 583.295V_e^{0.623}(2.18 + F_c), \quad e \in E^{\text{reac}} \quad (122)$$

The mass/heat exchange network superstructure model corresponds to a large-scale MINLP problem for which a nested MINLP decomposition based solution strategy developed in our earlier work is adopted (Ismail et al., 1999a).

Synthesis Examples

In this section, the synthesis problem for two classical reactive distillation examples is considered: the esterification of methanol and the production of MTBE. Synthesis alternatives for the ethyl acetate system are presented elsewhere (Ismail et al., 1999b). These examples aim to illustrate the ability of the synthesis framework to:

- capture the behavior of nonideal mixtures with detailed thermodynamic models and reaction kinetics
- capture the complex interaction of simultaneous reaction and separation
- identify the combination of reactive and nonreactive processes in process units
- determine a feasible separation/reaction structure

In the first example, the reaction is explicitly accounted for in the liquid-phase holdup, where the liquid volumetric holdup within each module is determined through the optimization. The second example shows that by explicitly considering the mass of catalyst as a variable, reactive heterogeneous systems can be accounted for when the reaction kinetics are given in terms of catalyst weight.

Utility costs of \$26.19 (U.S.)/kW·yr for cooling and \$137.27 (U.S.)/kW·yr for heating are utilized. For convenience in the presentation, and to reduce the size of the resulting mixed integer nonlinear programming problem, a number of further simplifying assumptions are made:

(i) Saturated liquid products are considered.

(ii) The system is at constant pressure. In the MTBE example the synthesis framework incorporates the system pressure as a variable to be determined by the optimization problem.

As discussed in Ismail et al. (1999a), such assumptions can be relaxed. In the following examples, the MINLP problems are solved using GAMS (Brooke et al., 1988), with solver CONOPT for the NLPs and CPLEX for the MIPs.

Example 1: esterification of methanol

Produced by the esterification of methanol by Eq. 1, methyl acetate is used in large amounts as an intermediate in the manufacture of a variety or polyesters. High purity methyl acetate is limited by reaction equilibrium and the formation of two binary minimum boiling azeotropes methyl acetate/methanol ($x_{MeAc} = 0.66$) and methyl acetate/water ($x_{MeAc} = 0.92$).

The quaternary system of acetic acid, methanol, water, and methyl acetate is nonideal in both the liquid and vapor phases. Dimerization of acetic acid in the vapor phase can be accounted for by the introduction of a correction factor z_i into the equilibrium relationship such that (Marek and Standart, 1954)

$$y_i z_i P_{\text{tot}} = x_i \gamma_i P_i^{\text{sat}} \quad (123)$$

where

$$z_A = \frac{1 + \left(1 + 4KP_A^{\text{sat}}\right)^{1/2}}{1 + \left[1 + 4KP_{\text{tot}} y_A (2 - y_A)\right]^{1/2}} \quad (124)$$

if A is the associating component (acetic acid) and

$$z_B = \frac{2\left\{1 - y_A + \left[1 + 4KP_{\text{tot}} y_A (2 - y_A)\right]^{1/2}\right\}}{(2 - y_A)\left\{1 + \left[1 + 4KP_{\text{tot}} y_A (2 - y_A)\right]^{1/2}\right\}} \quad (125)$$

if B is a nonassociating component. K is the dimerization equilibrium constant for the associating component (acetic acid) given by

$$\log_{10} K = -12.5454 + \frac{3{,}166}{T} \qquad (Pa^{-1})$$

The Wilson equation was utilized to capture the nonideality of the liquid phase, and all thermodynamic models and parameters are detailed in Table 5.

The liquid-phase reaction for methyl acetate synthesis can be catalyzed by inorganic acids like sulfuric acid or heterogeneously by strong acidic ion-exchange resins. In this work, the homogeneously catalyzed esterification is considered, where the rate of formation of ester is given by the following concentration based rate expression (Sawistowski and Pilavakis, 1979)

$$r = \frac{k[H^+]C_{\mathrm{AAcid}}C_{\mathrm{MeOH}}}{K_1 C_{\mathrm{H_2O}} + C_{\mathrm{MeOH}}} \qquad (\mathrm{kmol/m^3 \cdot s}) \qquad (126)$$

where the rate constant is given by

$$k = 1.2\times 10^6 \exp\left[\frac{-10{,}000}{RT}\right] \qquad (\mathrm{m^3/kmol \cdot s}) \quad (127)$$

and the equilibrium constant is expressed as a function of temperature

$$K_1 = \frac{\rho_{\mathrm{MeOH}}}{\left[0.11 + 0.0007043(T - 273.15)^{1.556}\right]} \qquad (128)$$

where ρ_{MeOH} is in kmol/m^3 to make K_1 dimensionless.

Consider the synthesis task for the production of 9.8 mol/s of 98% pure methyl acetate at 1 atm, given as raw products pure methanol and acetic acid. Ethylene glycol is available as a solvent and sulfuric acid as a homogeneous catalyst. A maximum mol fraction of sulfuric acid of 0.02 is allowed in each module, since high concentrations can cause problems such as corrosion and product contamination. A total of 20 liquid-vapor mass/heat exchangers are considered, 10 pure separation and 10 with combined separation/reaction, and 5 liquid-liquid mass/heat exchangers.

The synthesis task is driven by the minimization of annualized cost based on plant operation of 7,920 h/yr, including the cost of utilities, raw materials and a module cost based on its size

$$Z = \Sigma C_{cw} * Qc + \Sigma C_{\mathrm{steam}} * Qh + C_{\mathrm{AAcid}} * f_{\mathrm{feed,AAcid}} + C_{\mathrm{MeOH}} * f_{\mathrm{feed,MeOH}} + \Sigma y_{L-V} * \mathrm{Cost}_{L-V} + \Sigma y_{L-L} * \mathrm{Cost}_{L-L} \qquad (129)$$

Table 5. Methyl Acetate Production: Thermodynamic Properties

Component	$C1$	$C2$	$C3$	ΔG^f (kJ/kmol)	v_i m^3/mol
Acetic acid	9.51271	1,533.313	−50.851	-3.7405×10^5	57.54×10^{-6}
Methanol	10.20586	1,582.271	−33.434	-1.6242×10^5	40.73×10^{-6}
Methyl acetate	9.19013	1,157.63	−53.434	-3.2154×10^5	79.84×10^{-6}
Water	10.19620	1,730.63	−39.734	-2.2859×10^5	18.07×10^{-6}

$$\log P^{\mathrm{sat}} = C1 - \frac{C2}{C3 + T} \qquad \text{(Pa, K)}$$

Wilson Equation

$$\ln \gamma_i = 1 - \ln\left[\sum_j x_j \Lambda_{ij}\right] - \sum_k \frac{x_k \Lambda_{ki}}{\sum_j x_j \Lambda_{kj}}$$

$$\Lambda_{ij} = \frac{v_j}{v_i}\exp\left(\frac{-A_{ij}}{T}\right) \qquad A_{ii} = 0$$

Binary Interaction Parameters A_{ij} (K)

	Acetic acid	Methanol	Methyl acetate	Water
Acetic acid	0.0	−7.0931	−204.3598	2.0311
Methanol	11.8097	0.0	453.5853	41.6934
Methyl acetate	433.9473	−65.4667	0.0	352.5512
Water	403.1564	262.1529	982.5402	0.0

Pure Component Enthalpy
$H = AT + B$ (J/mol, K)

	Acetic acid	Methanol	Methyl acetate	Water
Vapor A	76.1687	48.7023	93.0998	34.1335
B	−22,964.9971	−14,650.5741	−28,102.0306	−10,185.52543
Liquid A	64.7570	126.7599	170.0476	80.3012
B	−41,942.0895	−77,009.7147	−84,201.9037	−68,066.8819

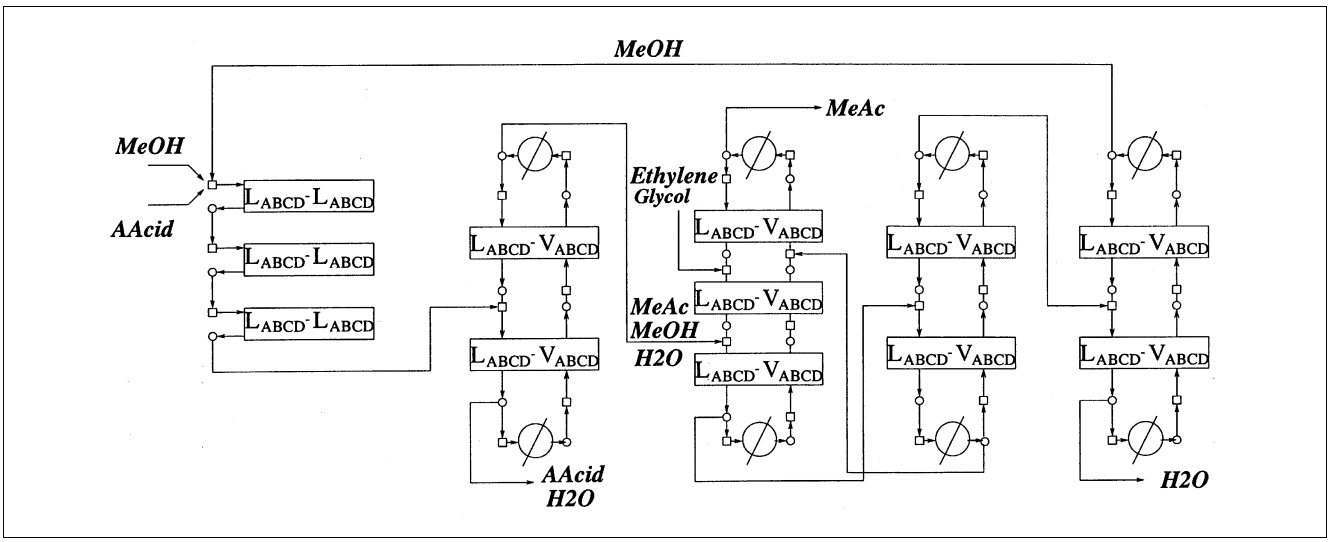

Figure 6. Methyl acetate production: initial structure.

where $C_{\text{AAcid}} = \$4.767$ (U.S.)/kmol, $C_{\text{MeOH}} = \$0.393$ (U.S.)/kmol and module costs Cost_{L-V} and Cost_{L-L} are given by Eqs. 121 and 122.

An initial structure of three liquid-liquid modules, nine pure separation liquid-vapor modules and eight pure heat exchanger modules in the configuration shown in Figure 6 is utilized (initial point I). This flowsheet can be generated using a conventional approach to process synthesis as described by Siirola (1995). Feed methanol and acetic acid enters a series of liquid-liquid modules representing a reactor, whereby reaction occurs in the liquid holdup. The exit stream consists of a mixture of the methyl acetate and water products and unreacted methanol and acetic acid, which is then separated in a series of distillation columns represented by the modules as illustrated. The first two liquid-vapor modules remove all the acetic acid and some water from the mixture as bottoms products. In a conventional industrial process, this would be further separated to recover all the acetic acid. The top product is directed to three liquid-vapor matches representing an extractive distillation column, whereby ethylene glycol is used to break up the homogeneous azeotropes to give the desired pure methyl acetate product. The bottoms product is then further separated to recover the glycol solvent which is recycled back. The remaining methanol-water mixture is then separated in a final distillation column to give pure methanol which is recycled back to the reactor and water.

Minimization of the annualized cost function (Eq. 129) results in the configuration shown in Figure 7, consisting of two liquid-vapor modules with liquid holdups (separation and reaction) in between two pure separation liquid-vapor modules, and two pure heat exchangers. The solution represents a double feed reactive distillation column with reactive and nonreactive sections, featuring a total cost of $\$1.5961 \times 10^6$ (U.S.)/yr, corresponding mainly to feed cost of $\$1.427 \times 10^6$ (U.S.)/yr, utility cost of $\$1.225 \times 10^5$ (U.S.)/yr, and module cost of $46,600 (U.S.)/yr. The bulk of the reaction occurs within the two middle modules featuring catalyst fraction of 0.02 and total extent of reaction of 9.604 mol/s. The top and bottom modules have no liquid holdup, and thus negligible reaction. In the top liquid-vapor module, separation of methyl acetate and acid is achieved, giving almost pure methyl acetate product. The bottom pure separation module separates methanol and water, purifying the water product. A similar solution is also obtained when starting from an initial configuration of a double feed reactive distillation column (similar to Figure 7) consisting of three separation-reaction-reaction liquid-vapor modules each with 20 m^3 liquid holdup in between four pure separation liquid-vapor modules and two pure heat exchangers (initial point II).

The results are utilized as inlet specifications for a simulation of a reactive distillation column assuming simultaneous chemical and physical equilibrium for verification. Each liquid-vapor module is assumed to correspond to six trays, with the module with the larger holdup to seven trays, giving a column with a total of 25 equilibrium trays. The reaction zone consists of 13 trays, and since the same reaction kinetics could

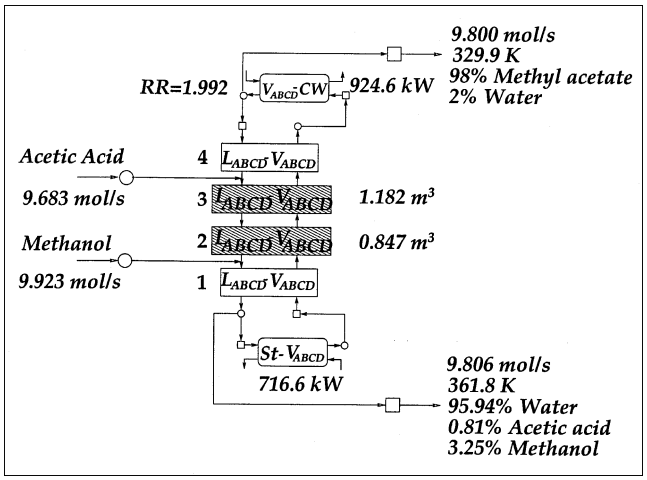

Figure 7. Methyl acetate production: 'optimal' configuration.

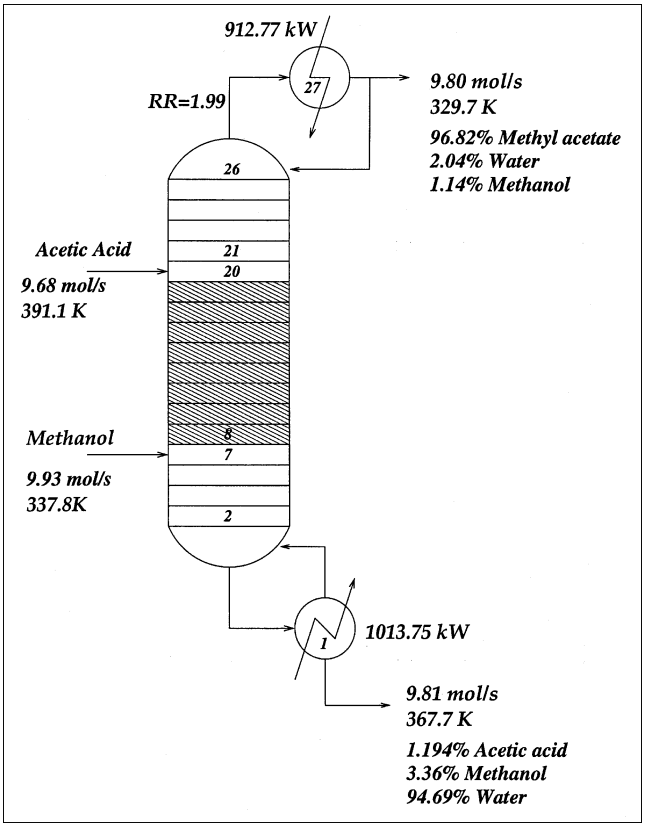

Figure 8. Methyl acetate production: Aspen simulation.

not be implemented, chemical equilibrium is assumed whereby (Barbosa and Doherty, 1988b)

$$K_{\text{eq}} = \prod_{i}^{C} \gamma_i x_i^{\nu_i} = 14.6 \tag{130}$$

The column is simulated using AspenPlus and the rigorous steady-state distillation module RADFRAC with the Redlich-Kwong/UNIQUAC property set (SYSOP2). The results are illustrated in Figure 8, with the reboiler and condenser duties of the Aspen model recalulated utilizing the same enthalpy correlations. A number of comments can be made:

- The reboiler within the modular model is a total reboiler with no mass exchange, and the liquid product is removed before being heated. The Aspen model features a partial reboiler which heats the product to its bubble point, resulting in a higher reboiler duty.
- Although detail is lost within the mass/heat exchangers, the main features of the reactive column are captured in four modules. This is shown in Figure 9 and Figure 10 where the temperature and liquid composition profiles are compared. Note that the liquid inlet and outlet module variables are plotted at the corresponding tray number within these plots (that is, liquid inlet to module 1 corresponds to liquid inlet to tray 7, outlet of module 4 to outlet of tray 21).

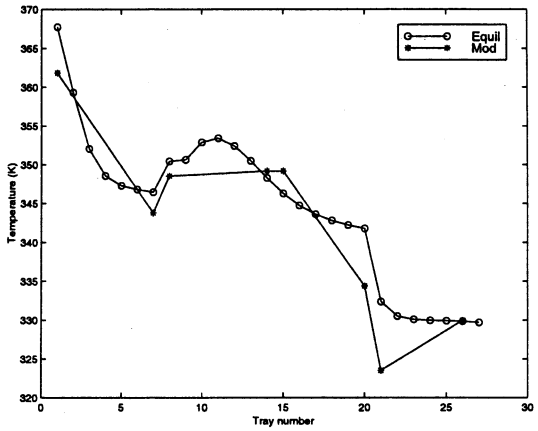

Temperature vs Tray Number

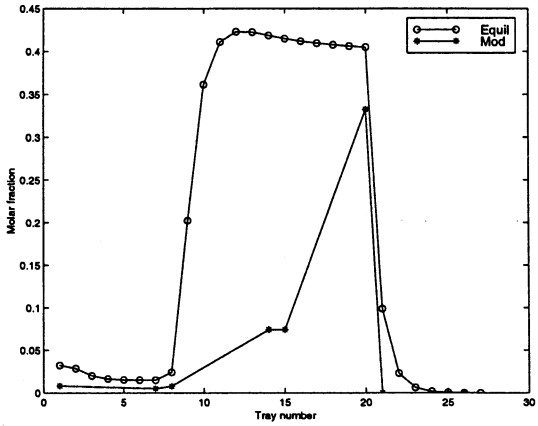

Acetic Acid Molar Fraction vs Tray Number

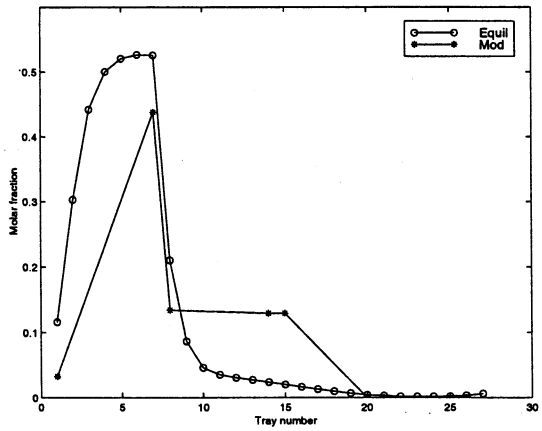

Methanol Molar Fraction vs Tray Number

Figure 9. Methyl acetate modular results vs. equilibrium simulation: Part A.

Example 2: Production of MTBE

The synthesis task for the production of 197 mol/s of at least 98% pure liquid MTBE is considered, with ion-exchange resin Amberlyst 15 available as catalyst. Raw materi-

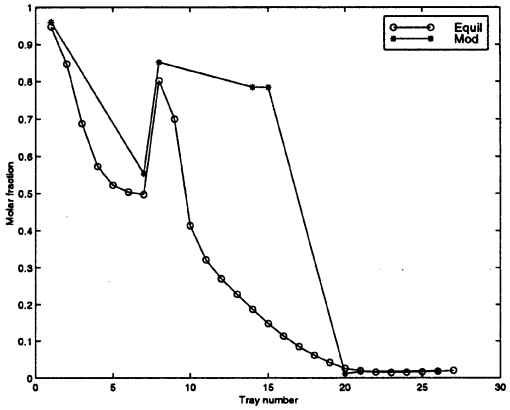

Methyl Acetate Molar Fraction vs Tray Number

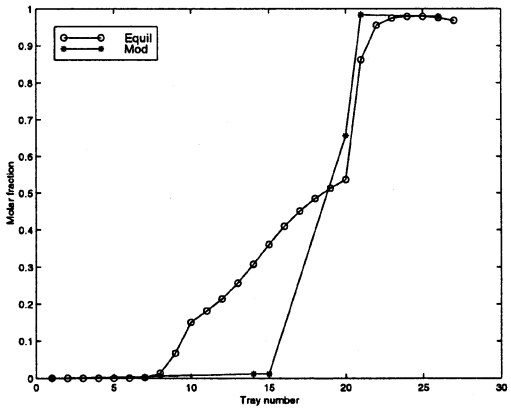

Water Molar Fraction vs Tray Number

Figure 10. Methyl acetate modular results vs. equilibrium simulation: Part B.

als are a pure liquid methanol and a saturated vapor isobutylene feed consisting of isobutylene $x_{IB} = 0.3558$ and n-butene inert $x_{NB_4} = 0.6442$. The feed flow rates and temperatures are variables to be determined. The methanol feed is constrained to be less than 200 mol/s to avoid multiple steady states and a maximum vapor flow rate of 3,000 mol/s around the mass/heat exchangers is enforced to constrain the equipment size (Eldarsi and Douglas, 1998b). Constant system pressure is considered. In this example, the system pressure is not fixed, but it is incorporated as a variable whose value will be determined by the minimization of the operating and the penalizing pseudo-capital cost as in the previous example, where

$$\text{Cost}(\$/\text{yr}) = \Sigma C_{cw} * Qc + \Sigma C_{\text{steam}} * Qh + C_{\text{MeOH}} * f_{\text{feed,MeOH}} + C_{\text{IB}} * f_{\text{feed},IB}, + \Sigma y_{L-V} * \text{Cost}_{L-V} \quad (131)$$

where $C_{\text{MeOH}} = \$0.393$ (U.S.)/kmol, $C_{IB} = \$0.767$ (U.S.)/kmol and Cost_{L-V} is given by Eq. 121 as a function of vapor flow rate with $H = 2$. A maximum of 10 pure separation and 10 combined separation/reaction liquid-vapor modules are allowed. The mass of catalyst within the module, if it exists, is considered on a dry-weight basis at a maximum mass of 2,000 kg per module.

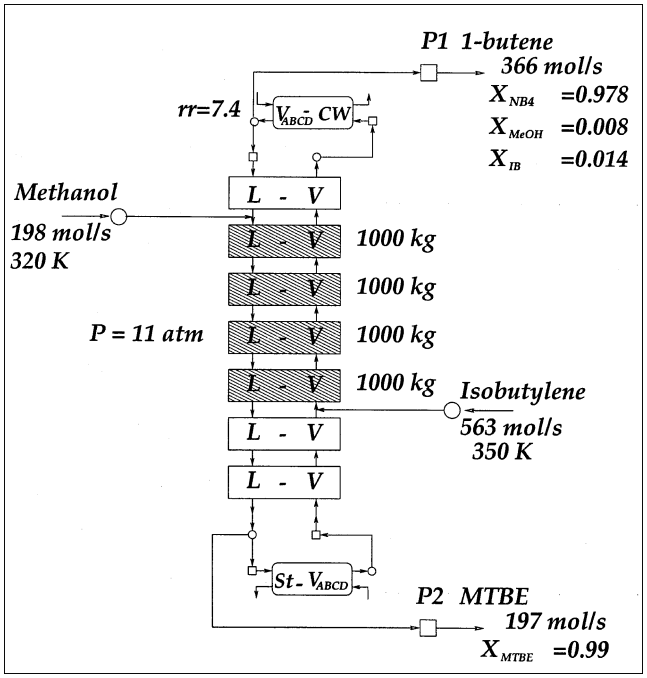

Figure 11. MTBE production: initial structure.

The initial structure is illustrated in Figure 11, similar to that reported in the open literature for the reactive distillation column for the synthesis of MTBE (Jacobs and Krishna, 1993), featuring seven liquid-vapor mass/heat exchangers and two pure heat exchangers. The four modules with simultaneous reaction and separation make up the reactive section with a total of 4,000 kg of catalyst. Minimization of the annualized cost function (Eq. 131) results in the configuration of modules as illustrated in Figure 12. The structure features four mass-/heat-transfer modules and two pure heat exchanger

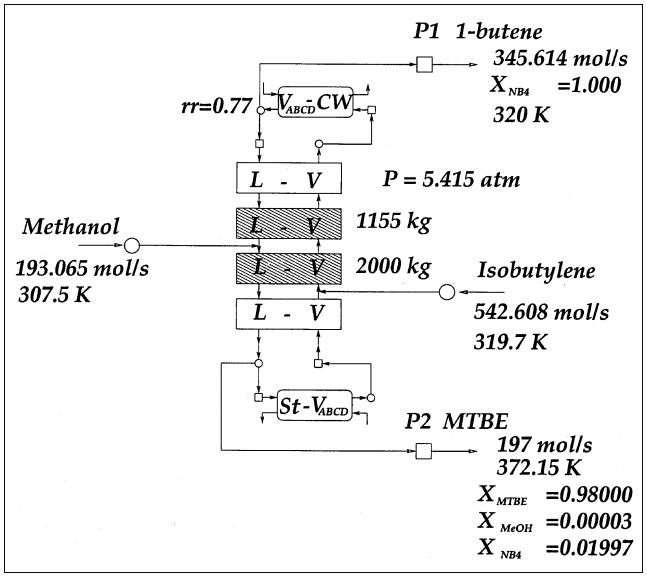

Figure 12. MTBE production: 'optimal' configuration.

models, in a configuration representing a reactive separation column. The reactive section is made up of two modules, featuring a total of 3,155 kg, whereby 197 mol/s of MTBE is generated. The pure separation module at the bottom of the unit separate the MTBE from the unreacted methanol, which is driven back into the reactive zone. Here, MTBE is transferred to the liquid phase, and methanol to the vapor phase. In the pure separation module at the top of the unit, the inert *n*-butene is transferred to the vapor phase to give pure inert distillate. This solution features a total cost of \$1.46755 $\times 10^7$ (U.S.)/yr, corresponding mainly to a feed cost of \$1.403$\times 10^7$ (U.S.)/yr, utility cost of \$5.843$\times 10^5$ (U.S.)/yr, and module cost of \$61,200 (U.S.)/yr. The resulting system data can be found in Figure 12.

Effects of system pressure

A note must be made here, regarding the very important role of pressure. The system pressure is determined by the optimization to be at 5.415 atm. This decrease (pressure of 11 atm in the initial structure) is driven by the objective function cost. The proposed framework proves that it is desirable to operate the column at a lower system pressure, when the latter is incorporated as an optimization variable, achieving lower heating and cooling duties (reducing the utilities required) and higher conversions of isobutene to MTBE.

Similar conclusions about the effects of lower system pressure were also remarked by Abufares and Douglas (1995) and Eldarsi and Douglas (1998a), who indicated that the importance of the system pressure in mainly due to its effect on the column temperature profile. The latter affects the reaction rate, the equilibrium, the ease of separation of the components and, in addition, the reflux ratio and the cooling and heating duties. To be more specific, decreasing the column pressure (and thus the column temperature), *initially*, decreases the MTBE synthesis reaction rate constant and the conversion of isobutene to MTBE. But, since the MTBE synthesis reaction is both reversible and exothermic with an equilibrium constant inversely proportional to the column temperature, a further decrease of the column pressure *ultimately* results in higher rates of reaction and higher isobutene conversions. This is due to the proportional relation of the equilibrium constant to the distance from chemical equilibrium, which, in turn, is proportional to the MTBE synthesis reaction rate. Therefore, from the above, it can be seen that decreasing the column pressure leads to higher MTBE synthesis reaction rates, to higher reactants' conversions, and to lower reactants' carryover in the column. Consequently, lower vapor flow rates and reflux ratios are achieved, resulting in lower condenser and reboiler duties and lower operating cost. In conclusion, the above serve as a theoretical verification of our results which indicate that in order to achieve optimal operation of the MTBE reactive distillation column, with respect to the minimization of the operating cost, the system should be operated at lower pressures.

Concluding Remarks

In this work, we utilize the phenomena of the system within a modular network superstructure to generate process alternatives for separation/reactive systems. The basis of this representation are the driving force constraints, which are able to accurately characterize the complex mass-transfer phenomena occurring when we have simultaneous separation and reaction. With no prepostulation of process units, structures and mass-transfer patterns, rather than detailed designs, can be captured. Reactive azeotropes, whose theoretical existence has been experimentally confirmed, are equilibrium phenomena where the rate of vaporization and condensation, coupled with the reaction rate, occur without change of composition in each phase. Within the mass-/heat-transfer module, it is believed that their existence can be predicted as a limit of mass transfer enforced by the driving force constraints, similar to that for homogeneous azeotropes as shown in our earlier work (Ismail et al., 1999a). The ability of the framework to capture and evaluate reactive azeotropes and multiple steady states is under current investigation.

Table 6. Computational Details of the Synthesis Examples

Synthesis Example		No. of Iterations	CPU
Methyl Acetate	Initial point (I)	15	7,356
	Initial point (II)	8	4,094
MTBE		9	2,407

The emphasis of the work so far has concentrated on demonstrating the modeling/representation validity of the proposed modular approach. While the computational effort for solving the examples presented here has been rather reasonable (Table 6), arguably the inherent logic that exists in the synthesis model has not been fully exploited. Here, advances in logic-based mixed integer optimization techniques (Grossmann and Hooker, 1999) are of vital importance.

The example of MTBE, in particular, considers the system pressure as an optimization variable, which can play an important role in combined separation/reaction systems. The effects of pressure are investigated within the proposed framework and are proved to be in accord with the MTBE reactive distillation literature.

Finally, heat integration can be considered as part of the synthesis problem by considering stream-stream heat exchanger matches in addition to the utility-stream matches that are considered in this work, and accounting for all the interconnections between the exchanger mixers and splitters. Extending the model to encompass such alternatives can be readily envisaged, albeit at the expense of considerably increasing the size of the resulting MINLP. This is an issue of current research.

Acknowledgments

Financial support from the European Communities, under contract JOE3-CT97-0085 (HY-SEP project) is greatly acknowledged. The authors would also like to acknowledge Dr. Katerina Papalexandri and Mr. Dimitris Orfanidis for their theoretical contributions to this work, and the reviewers for providing useful comments on an earlier draft of the article.

Notation

a_i = liquid-phase activity $a_i = \gamma_i x_i$
C_{cw} = cooling utility cost
C_{steam} = heating utility cost
f = molar flow rate

h = enthalpy
M_{cat} = mass of catalyst
n_i = number of moles
P_{tot} = total system pressure
P_i^{sat} = saturated vapor pressure
Qh = heating duty
Qc = cooling duty
r_k = rate of reaction
R = gas constant
T = temperature
V = liquid volume holdup
$\bar{V}$ = liquid volumetric flow rate
x_i = molar fraction

Greek letters

ϵ_k = extent of reaction
γ_i = activity coefficient
μ_i = component chemical potential
ν_{ik} = stoichiometric coefficient
ϕ_i = fugacity coefficient
ρ_i = component liquid density
ρ_m = liquid mixture density
θ = active residence time

Subscripts

e = module
i, j = component
k = reaction
n = initial stream
p = product stream
s = superstructure stream

Superscripts

L = liquid phase
V = vapor phase
LI = liquid inlet stream
LO = liquid outlet stream
VI = vapor inlet stream
VO = vapor outlet stream

Literature Cited

Abufares, A. A., and P. L. Douglas, "Mathematical Modelling and Simulation of an MTBE Catalytic Distillation Process Using SpeedUp and Aspen Plus," *Trans. IChemE Part A*, **73**, 3 (1995).

Al-Jarallah, A. D., M. A. B. Siddiqui, and K. K. Lee, "Kinetics of Methyl Tertiary Butyl Ether Synthesis catalyzed by Ion Exchange Resin," *J. Chem. Eng. Data*, **66**, 802 (1988).

Barbosa, D., and M. F. Doherty, "Design and Minimum Reflux Calculations for Double Feed Multicomponent Reactive Distillation Columns," *Chem. Eng. Sci.*, **43**, 2377 (1988a).

Barbosa, D., and M. F. Doherty, "Design and Minimum Reflux Calculations for Single Feed Multicomponent Reactive Distillation Columns," *Chem. Eng. Sci.*, **43**, 1523 (1988b).

Barbosa, D., and M. F. Doherty, "The Influence of Equilibrium Chemical-Reactions on Vapor-Liquid Phase Diagrams," *Chem. Eng. Sci.*, **43**, 529 (1988c).

Barbosa, D., and M. F. Doherty, "The Simple Distillation of Homogeneous Reactive Mixtures," *Chem. Eng. Sci.*, **43**, 541 (1988d).

Brooke, A., D. Kendrick, and A. Meeraus, *GAMS: A User Guide*, The Scientific Press, San Francisco (1988).

Ciric, A. R., and D. Gu, "Synthesis of Nonequilibrium Reactive Distillation Processes by MINLP Optimization," *AIChE J.*, **40**, 1479 (1994).

Colombo, F., L. Cori, and P. Delogu, "Equilibrium Constant for the Methyl tert-Butyl Ether Liquid-Phase Synthesis by Use of UNIFAC," *Ind. Eng. Chem. Fundam.*, **22**, 219 (1983).

Doherty, M. F., and G. Buzad, "Reactive Distillation by Design," *Trans. IChemE Part A*, **70**, 448 (1992).

Douglas, J. M., "A Hierarchical Decision Procedure for Process Synthesis," *AIChE J.*, **31**, 353 (1985).

Eldarsi, H. S., and P. L. Douglas, "Methyl-Tert-Butyl-Ether Catalytic Distillation Column: I. Multiple Steady State," *Trans. IChemE Part A*, **76**, 509 (1998a).

Eldarsi, H. S., and P. L. Douglas, "Methyl-Tert-Butyl-Ether Catalytic Distillation Column: II. Optimization," *Trans. IChemE Part A*, **76**, 517 (1998b).

Grossmann, I. E., and J. Hooker, "Logic Based Approaches for Mixed Integer Programming Models and their Application in Process Synthesis," *FOCAPD '99 Technical Program and Reprints*, Colorado, USA (1999).

Hauan, S., "On the Behaviour of Reactive Distillation Systems," PhD Diss., Norwegian University of Science and Technology (NTNU), Trondheim, Norway (1998).

Hauan, S., and K. M. Lien, "A Phenomena Based Design Approach to Reactive Distillation," *Trans. IChemE Part A*, **76**, 396 (1998).

Hauan, S., T. Hertzberg, and K. Lien, "Why Methyl Tert-butyl Ether by Reactive Distillation May Yield Multiple Solutions," *Ind. Eng. Chem. Res.*, **34**, 987 (1995).

Higler, A., R. Taylor, and R. Krishna, "Modeling of a Reactive Separation Process Using a Nonequilibrium Stage Model," *Comput. Chem. Eng.*, **22**, S111 (1998).

Ismail, S. R., E. N. Pistikopoulos, and K. P. Papalexandri, "Separation of Nonideal Mixtures Based on Mass/Heat Exchange Principles. The Entrainer Selection and Sequencing Problem," *Comput. Chem. Eng.*, **21**, S211 (1997).

Ismail, S. R., E. N. Pistikopoulos, and K. P. Papalexandri, "Modular Representation Synthesis Framework for Homogeneous Azeotropic Separation," *AIChE J.*, **45**, 1701 (1999a).

Ismail, S. R., E. N. Pistikopoulos, and K. P. Papalexandri, "Synthesis of Reactive and Combined Reactor/Separation Systems Utilising a Mass/Heat Exchange Module," *Chem. Eng. Sci.*, **54**(13-14), 2721 (1999b).

Jacobs, R., and R. Krishna, "Multiple Solutions in Reactive Distillation for Methyl tert-Butyl Ether Synthesis," *Ind. Eng. Chem. Res.*, **32**, 1706 (1993).

Lakshmanan, A., and L. T. Biegler, "Synthesis of Optimal Chemical Reactor Networks with Simultaneous Mass Integration," *Ind. Eng. Chem. Res.*, **35**, 4523 (1996).

Marek, J., and G. Standart, "Vapor-Liquid Equilibria in Mixtures Containing an Associating Substance: I. Equilibrium Relationships for Systems with an Associating Component," *Colln. Czech. chem. Commun., Engl. Edn.*, **19**, 1074 (1954).

Nisoli, A., M. F. Malone, and M. F. Doherty, "Attainable Regions for Reaction with Separation," *AIChE J.*, **43**, 374 (1997).

Okasinski, M. J., and M. F. Doherty, "Thermodynamic Behaviour of Reactive Azeotropes," *AIChE J.*, **43**, 2227 (1997).

Okasinski, M. J., and M. F. Doherty, "Design Method for Kinetically Controlled, Staged Reactive Distillation Columns," *Ind. Eng. Chem. Res.*, **37**, 2821 (1998).

Orfanidis, D. P., "Generalized Modular Representation Framework for Process Synthesis-Reactive Distillation Systems," M.Sc. Diss., Imperial College of Science, Technology and Medicine, London (1997).

Papalexandri, K. P., and E. N. Pistikopoulos, "Generalized Modular Representation Framework for Process Synthesis," *AIChE J.*, **42**, 1010 (1996).

Perez-Cisneros, E. S., R. Gani, and M. L. Michelsen, "Reactive Separation Systems: I. Computation of Physical and Chemical Equilibrium," *Chem. Eng. Sci.*, **52**, 527 (1997).

Rahim Ismail, S., "A Generalised Modular Framework for the Synthesis of Nonideal Separation and Reactive Separation Processes," PhD Diss., Imperial College of Science, Technology and Medicine, London (1998).

Rehfinger, A., and U. Hoffmann, "Kinetics of Methyl Tertiary Butyl Ether Liquid Phase Synthesis Catalyzed by Ion Exchange Resin: I. Intrinsic Rate Expression in Liquid Phase Activities," *Chem. Eng. Sci.*, **45**(6), 1605 (1990).

Sawistowski, H., and P. A. Pilavakis, "Distillation with Chemical Reaction in a Packed Column," *I. Chem. E. Symp. Ser.*, **56**, 42 (1979).

Siirola, J. J., "An Industrial Perspective on Process Synthesis," *Foundations of Computer-Aided Process Design*, L. T. Biegler and M. F. Doherty, eds., AIChE Symp. Ser., No. 304, Vol. 91, 222 (1995).

Smith, E. M., "On the Optimal Design of Continuous Processes," PhD Diss., Imperial College of Science, Technology and Medicine, London (1996).

Ung, S., and M. F. Doherty, "Necessary and Sufficient Conditions for Reactive Azeotropes in Multireaction Mixtures," *AIChE J.*, **41**, 2383 (1995a).
Ung, S., and M. F. Doherty, "Synthesis of Reactive Distillation Systems with Multiple Equilibrium Chemical Reactions," *Ind. Eng. Chem. Res.*, **34**, 2555 (1995b).

Appendix A: Derivation of $\partial\epsilon/\partial n_i^L$

MTBE production

The extent of reaction for this system is given by (Orfanidis, 1997)

$$\epsilon = r * \theta * M_{\text{cat}} \tag{A1}$$

where r is the reaction rate, M_{cat} is the mass of catalyst on a dry basis, and θ is the active residence time, that is, time the mixture spends reacting in the liquid holdup. In a module, the residence time is calculated as the contact time of the mixture within the liquid holdup, which is evaluated by

$$\theta = \frac{\text{Volume of liquid holdup in m}^3}{\text{Volumetric Flow rate of liquid through holdup}}$$

$$= \frac{V}{\overline{V}} = \frac{n_{\text{tot}}^L/\rho_m^L}{f^L/\rho_m^L} \tag{A2}$$

$$= \frac{n_{tot}^L}{f^L} \tag{A3}$$

where $n_{\text{tot}}^L = \Sigma_i n_i^L$

Substituting for the rate (Eq. 20) and residence time (Eq. A3) (dropping the superscript L on n_i^L)

$$\epsilon = \left[\frac{\gamma_{\text{IB}} x_{\text{IB}}}{\gamma_{\text{MeOH}} x_{\text{MeOH}}} - \frac{1}{Ka}\frac{\gamma_{\text{MTBE}} x_{\text{MTBE}}}{\gamma_{\text{MEOH}}^2 x_{\text{MeOH}}^2 x_{\text{MeOH}}^2}\right]\frac{n_{\text{tot}}}{f} kM_{\text{cat}}$$

$$= \left[\frac{\gamma_{\text{IB}} n_{\text{IB}} n_{\text{tot}}}{\gamma_{\text{MeOH}} n_{\text{MeOH}}} - \frac{1}{Ka}\frac{\gamma_{\text{MTBE}} n_{\text{MTBE}} n_{\text{tot}}^2}{\gamma_{\text{MeOH}}^2 n_{\text{MeOH}}^2}\right]\left(\frac{kM_{\text{cat}}}{f}\right) \tag{A4}$$

To obtain an analytical expression for $\partial\epsilon/\partial n_i$, this expression must be differentiated with respect to each component holdup n_i, keeping all $n_{j\neq i}$, T and P constant. The last bracketed term is constant, and we assume that the contribution of $\partial\gamma_i/\partial n_i \approx 0$ and can be neglected. Differentiating with respect to n_{IB}

$$\frac{\partial\epsilon}{\partial n_{\text{IB}}} = \left[\frac{\gamma_{\text{IB}}}{\gamma_{\text{MeOH}} n_{\text{MeOH}}}\frac{(\partial n_{\text{IB}} n_{\text{tot}})}{\partial n_{\text{IB}}} - \frac{1}{Ka}\frac{\gamma_{\text{MTBE}}\eta_{\text{MTBE}}}{\gamma_{\text{MeOH}}^2 n_{\text{MeOH}}^2}\frac{\partial\left(n_{\text{tot}}^2\right)}{\partial n_{\text{IB}}}\right]\left(\frac{kM_{\text{cat}}}{f}\right)$$

$$= \left[\frac{\gamma_{\text{IB}}}{\gamma_{\text{MeOH}} n_{\text{MeOH}}}(n_{\text{IB}} + n_{\text{tot}}) - \frac{1}{Ka}\frac{\gamma_{\text{MTBE}} n_{\text{MTBE}}}{\gamma_{\text{MeOH}}^2 n_{\text{MeOH}}^2} 2n_{\text{tot}}\right] \times\left(\frac{kM_{\text{cat}}}{f}\right)$$

$$= \left[\frac{\gamma_{\text{IB}}}{\gamma_{\text{MeOH}} x_{\text{MeOH}}} + \frac{\gamma_{\text{IB}} x_{\text{IB}}}{\gamma_{\text{MeOH}} x_{\text{MeOH}}} - \frac{2}{Ka}\frac{\gamma_{\text{MTBE}} x_{\text{MTBE}}}{\gamma_{\text{MeOH}}^2 x_{\text{MeOH}}^2}\right] \times\left(\frac{kM_{\text{cat}}}{f}\right) \tag{A5}$$

Similar treatment for MeOH and MTBE gives Eqs. 24–25. For inerts (n-butene), $\partial\epsilon/\partial n_{\text{NB4}}^L = 0$.

Methyl acetate

At steady state, the extent of reaction ϵ is given by

$$\epsilon = r * V * \theta \tag{A6}$$

Substituting for the reaction rate (Eq. 126), this becomes

$$\epsilon = \frac{k[H^+] n_{\text{AAcid}}^L n_{\text{MeOH}}^L \theta}{K_1 n_{\text{H}_2\text{O}}^L + n_{\text{MeOH}}^L} \tag{A7}$$

where n_i^L is the molar liquid holdup of component i in the reacting liquid mixture and $[H^+]$ is the concentration of catalyst hydrogen ions.

Substituting for θ (Eq. A3), Eq. A7 then becomes

$$\epsilon = \frac{k[H^+] n_{\text{AAcid}}^L n_{\text{MeOH}}^L n_{\text{TOT}}^L}{f^L\left(K_1 n_{\text{H}_2\text{O}}^L + n_{\text{MeOH}}^L\right)} \tag{A8}$$

To differetiate this expression, the catalyst concentration is taken to be independent of changes in molar holdup of the reacting system components. Differentiating with respect to the molar holdup of acetic acid, (dropping the superscript L)

$$\frac{\partial\epsilon}{\partial n_{\text{AAcid}}} = \frac{k[H^+]}{f\left(K_1 n_{\text{H}_2\text{O}} + n_{\text{MeOH}}\right)}\left(n_{\text{MeOH}} n_{\text{TOT}} + n_{\text{AAcid}} n_{\text{MeOH}}\right)$$

$$= \frac{k[H^+]}{f\left(K_1 x_{\text{H}_2\text{O}} + x_{\text{MeOH}}\right) n_{\text{TOT}}}\left(x_{\text{MeOH}} n_{\text{TOT}}^2 + x_{\text{AAcid}} x_{\text{MeOH}} n_{\text{TOT}}^2\right)$$

$$= \frac{k[H^+] n_{\text{TOT}}}{f\left(K_1 x_{\text{H}_2\text{O}} + x_{\text{MeOH}}\right)} x_{\text{MeOH}}(1 + x_{\text{AAcid}}) \tag{A9}$$

Differentiation with respect to the other components in a similar fashion leads to the following expressions

$$\frac{\partial\epsilon}{\partial n_{\text{MeOH}}} = \frac{k[H^+] n_{\text{TOT}}}{f\left(K_1 x_{\text{H}_2\text{O}} + x_{\text{MeOH}}\right)^2} x_{\text{AAcid}}\left(x_{\text{MeOH}}^2 + K_1 x_{\text{H}_2\text{O}} + K_1 x_{\text{H}_2\text{O}} x_{\text{MeOH}}\right) \tag{A10}$$

$$\frac{\partial\epsilon}{\partial n_{\text{MeAc}}} = \frac{k[H^+] n_{\text{TOT}}}{f\left(K_1 x_{\text{H}_2\text{O}} + x_{\text{MeOH}}\right)} x_{\text{AAcid}} x_{\text{MeOH}} \tag{A11}$$

$$\frac{\partial\epsilon}{\partial n_{\text{H}_2\text{O}}} = \frac{k[H^+] n_{\text{TOT}}}{f\left(K_1 x_{\text{H}_2\text{O}} + x_{\text{MeOH}}\right)^2} x_{\text{AAcid}} x_{\text{MeOH}}\left(K_1 x_{\text{H}_2\text{O}} + x_{\text{MeOH}} - K_1\right) \tag{A12}$$

Appendix B: Derivation of Module Cost

Guthrie's costing correlation for a pressure vessel is given by

$$\text{Installed Cost, \$} = \left(\frac{M\&S}{280}\right) 101.9 D^{1.066} H^{0.802} (2.18 + F_c) \tag{B1}$$

where
D = diameter in ft
H = height in ft
$F_c = F_m F_p$, function of shell material

A liquid-vapor match with inlet and outlet flows is essentially a separator and is estimated to be part of a column. The cost of such a module is proportional to the vapor flow rate through it, the amount of separation involved, and the molar holdup. Estimating liquid-vapor mass/exchanging modules as part of or a column, the diameter can be calculated by allowing the vapor velocity to be 80% of the flooding velocity. The flooding velocity can be approximated by (Douglas, 1985)

$$v_{\text{flood}} / \rho_{g,m} = \text{constant} = 1.5 \tag{B2}$$

where v_{flood} is in ft/s and $\rho_{g,m}$ is the vapor density in lb/ft^3. The cross-sectional area of the unit is calculated by

$$A = \frac{\pi D^2}{4} = \frac{\text{Vapor volumetric flow rate}}{\text{Vapor velocity}} \tag{B3}$$

The vapor volumetric flow rate is calculated from the division of the vapor molar flow rate by the vapor molar density. Taking the vapor velocity to be 80% of the flooding velocity and allowing for 12% of the separator area to be taken up by internals, Eq. B3 can be rearranged to give

$$D = 0.2734 \left(\frac{MW^V}{\rho^V}\right)^{0.25} \sqrt{f^V} \tag{B4}$$

where f_V is the vapor flow rate in kmol/h, MW^V the vapor mixture molar mass in g/mol and ρ^V the vapor mixture density in mol/m^3 (easily estimated assuming an ideal gas).

For a liquid-vapor module, H is the equivalent height to a separator is thus a function of the amount of mass transfer taking place within the module and the liquid holdup. Equation B4 is utilized with

$$H = 2 + \frac{4V}{\pi D^2} \tag{B5}$$

Using an $M\&S$ value of 1,000 and taking $1.066 \approx 1$, from Eq. B1 the cost of the liquid-vapor module can thus be approximated by

$$\text{Cost}_{L-V}(\$) = 99.507 \left(\frac{MW^V}{\rho^V}\right)^{0.25} \sqrt{f^V} H^{0.802} (2.18 + F_c) \tag{B6}$$

where H (ft) is determined from Eqs. B4 and B5 and $F_c = 1$ or $F_c = 1.15$ for carbon steel vessels of pressures up to 3.4 atm or 13.6 atm, respectively. It is noted that this cost function may not always be realistic, for example, it is not able to differentiate between a section operating at minimum and higher reflux ratio. However, it is able to give an approximation of the costs of liquid-vapor modules as a function of its size.

A liquid-liquid match with one inlet and outlet with reaction is approximated as part of or a whole reactor. The cost of the module is proportional to the volume of the liquid holdup and/or volume of the catalyst if present (V). Using the cost correlation in (Eq. B1) as a basis, some geometry must be assumed to calculate D and H. Assuming a cylindrical vessel with a height to diameter ratio of 6, the volumetric holdup of the module is given by

$$V = \frac{\pi D^2}{4} H = \frac{6\pi D^3}{4} \tag{B7}$$

Rearranging for the diameter

$$D = \left(\frac{2V}{3\pi}\right)^{1/3} \tag{B8}$$

Note that

$$D^{1.066} H^{0.802} = 6^{0.802} D^{1.868} = 6^{0.802} \left(\frac{2V}{3\pi}\right)^{0.623} = 1.602 V^{0.623}$$

From Eq. B1 using an $M\&S$ value of 1,000, the expression is simplified to

$$\text{Cost}_{L-L}(\$) = 583.295 V^{0.623} (2.18 + F_c) \tag{B9}$$

where V is in ft^3 and $F_c = 1$ or $F_c = 1.15$ depending on the pressure.

Manuscript received Dec. 15, 1998, and revision received July 17, 2000.